JOURNAL OF MATERIALS SCIENCE 29 (1994) 2579–2604

An approach to the formation and growth of new phases with application to polymer crystallization: effect of finite size, metastability, and Ostwald's rule of stages

A. KELLER, M. HIKOSAKA*, S. RASTOGI‡, A. TODA§, P. J. BARHAM, G. GOLDBECK-WOOD
H. H. Wills Physics Laboratory, University of Bristol, Tyndall Avenue, Bristol BS8 ITL, UK

This article aims to link the *mainstream* subject of chain-folded polymer crystallization with the rather speciality field of extended-chain crystallization, the latter typified by the crystallization of polyethylene (PE) under pressure. Issues of wider generality are also raised for crystal growth, and beyond for phase transformations. The underlying new experimental material comprises the prominent role of metastable phases, specifically the mobile hexagonal phase in polyethylene which can arise in preference to the orthorhombic phase in the phase regime where the latter is the stable regime, and the recognition of "thickening growth" as a primary growth process, as opposed to the traditionally considered secondary process of thickening. The scheme relies on considerations of crystal size as a thermodynamic variable, namely on melting-point depression, which is, in general, different for different polymorphs. It is shown that under specifiable conditions phase stabilities can invert with size; that is a phase which is metastable for infinite size can become the stable phase when the crystal is sufficiently small. As applied to crystal growth, it follows that a crystal can appear and grow in a phase that is different from that in its state of ultimate stability, maintaining this in a metastable form when it may or may not transform into the ultimate stable state in the course of growth according to circumstances. For polymers this intermediate initial state is one with high-chain mobility capable of "thickening growth" which in turn ceases (or slows down) upon transformation, when and if such occurs, thus "locking in" a finite lamellar thickness. The complete situation can be represented by a P, T, $1/l$ ($l \equiv$ crystal thickness) phase-stability diagram which, coupled with kinetic considerations, embodies all recognized modes of crystallization including chain-folded and extended-chain type ones. The task that remains is to assess which applies under given conditions of P and T. A numerical assessment of the most widely explored case of crystallization of PE under atmospheric pressure indicates that there is a strong likelihood (critically dependent on the choice of input parameters) that crystallization may proceed via a metastable, mobile, hexagonal phase, which is transiently stable at the smallest size where the crystal first appears, with potentially profound consequences for the current picture of such crystallization. Crystallization of PE from solution, however, would, by such computations, proceed directly into the final stage of stability, upholding the validity of the existing treatments of chain-folded crystallization. The above treatment, in its wider applicability, provides a previously unsuspected thermodynamic foundation of Ostwald's rule of stages by stating that phase transformation will always start with the phase (polymorph) which is stable down to the smallest size, irrespective of whether this is stable or metastable when fully grown. In the case where the phase transformation is nucleation controlled, a ready connection between the kinetic and thermodynamic considerations presents itself, including previously invoked kinetic explanations of the stage rule. To justify the statement that the crystal size can control the transformation between two polymorphs, a recent result on 1-4-poly-*trans*-butadiene is invoked. Furthermore, phase-stability conditions for wedge-shaped geometries are considered, as raised by current experimental material on PE. It is found that inversion of phase stabilities (as compared to the conditions pertaining for parallel-sided systems) can arise, with consequences for

* Present address: Department of Materials Science and Engineering, Faculty of Engineering, Yamagata University, Yonezawa, 992 Japan.
‡ Present address: Department of Polymer Technology, Eindhoven Technical University, 5600 MB Eindhoven, The Netherlands.
§ Present address: Department of Physics, Kyoto University, Kyoto 606-01, Japan.

0022–2461

our scheme of polymer crystallization and with wider implications for phase transformations in tapering spaces in general. In addition, in two of the Appendices two themes of overall generality (arising from present considerations for polymers) are developed analytically; namely, the competition of nucleation-controlled phase growth of polymorphs as a function of input parameters, and the effect of phase size on the triple point in phase diagrams. The latter case leads, *inter alia* to the recognition of previously unsuspected singularities, with consequences which are yet to be assessed.

1. Introduction

1.1. Motivation and scope

In this paper we present a scheme prompted by recent experimental studies on polymer crystallization under hydrostatic pressure – initiated by one of us (MH) in Tokyo (and currently in Yamagata) and subsequently extended by association with our Bristol Laboratory. The factual material is in the process of being reported separately elsewhere [1–4]. As such, new experimental results will not be reported nor any new theory *per se*, but this paper is meant to serve as a map for tracing the course of phase transformations in general and the course of chain-folded-polymer crystal growth in particular. Some links, hitherto unnoticed, between the thermodynamics and kinetics of phase transformations have been recognized, which we believe will be of wide-ranging relevance. Specifically, two factors have emerged in the course of the experimental works referred to above which were found to have a controlling influence on the crystallization processes in those experiments: metastable phases as the primary products of crystallization, and the size dependence of phase stability. Neither of these are new in themselves, yet their combination leads to new considerations, which (following the preliminary announcement in a conference paper [5]) are the subject of this paper. These two factors are taken in turn.

The role of metastability in phase transformations was recognized in the last century, and it is embodied in Ostwald's rule of stages, which states that phase transformations will always proceed through stages of metastable states whenever such metastable states exist. This rule is empirical, yet it is widely observed in phase transformations. In fact it also emerges from the data by Bassett and Turner [6, 7] who first observed that polyethylene (PE) can pass through a metastable phase first, when crystallized under elevated pressure. This latter effect has re-emerged even more forcibly in our own renewed works on this subject, placing the whole issue of the importance of the role of metastability in a rather heightened profile.

The second factor, the role of the phase size, is of course long familiar in the form of boiling-point and melting-point depressions etc. due to limited phase dimensions, and it is expressed quantitatively by the Thomson–Gibbs equation. Accordingly, a phase of small dimensions is less stable than one of larger size which is of otherwise identical internal structure. It follows that in this case we have size-determined metastability also applying to phase types which, for infinite size, would be in a state of absolute stability. In this case there will be a trend for redistribution (growth) of phase sizes embodied by the concept of Ostwald ripening. Again, the role of this size-determined metastability, and specifically the size-induced depression of phase transition, has taken on a special significance in our latest experimental works on pressure-induced polymer crystallization. When applying such considerations, not only to one particular phase, but also to polymorphic phases which are in kinetic competition with each other, new interrelations were perceived, which proved helpful in the interpretation of our crystal-growth results, and offered some new prospects, we maintain, for visualizing phase transformations generally. It is to be noted that given two or several polymorphs, only one can be stable, in general all the others must be metastable. The two issues, the role of "true" metastability and that of size-dependent stability merge at this point. This joining up of the two issues, each separately familiar has been the motivation for the scheme presented in this paper.

For the polymer-crystallization field itself, the scheme should serve a special unifying function. Namely, in the case of PE the most widely studied substance serving as model for polymer crystallization, the subject has so far been subdivided into two streams. (i) Chain-folded crystallization from melts and solutions under atmospheric pressure, which we would term the *mainstream*; and (ii) chain-extended crystallization occurring under elevated pressure, which we would here term the 'speciality stream'. There are only rather tenuous connections between (i) and (ii). The scheme presented in this paper should help to provide a unifying umbrella by creating a map in which both of these so far largely separate streams have their assigned place. Further, and even more importantly, this "map" should help in the search for both the boundaries and interconnections between the two areas of crystallization behaviour. A specific numerical computation has been added to show the way.

While within the above framework of the combined effects of phase-size determined and "true" metastability we shall also be invoking special shapes, such as the wedge shape impressed upon us by observation. This, as shown, leads us to some rather unexpected insights which are likely to be of wider relevance to phase transformations within confined tapering spaces.

A brief inclusion of experimental material on a polymer other than PE, poly-1–4-*trans*-butadiene, should set an example for the usefulness of the scheme to an as yet new situation involving the effect of size (in fact, a direct demonstration of the effect of size on

crystal–crystal transformation) and not necessarily requiring pressure for its own sake.

Finally, in the light of all the above, a previously unnoticed, but in retrospect self-evident, connection between thermodynamics (stability) and kinetics (rate) has become apparent which, amongst much else, has enabled the original Ostwald stage rule to be reassessed from a more timely and comprehensive perspective.

1.2. Experimental background for polymer crystallization

For self-contained reading the relevant experimental findings, together with its essential precedents from [1–4] will be briefly summarized.

As is known, PE normally crystallizes in the orthorhombic (o) crystal structure forming chain-folded lamellae of thickness, (l), remaining constant during continuing lateral growth; this is the principal feature of all *mainstream* crystallization studies. Under elevated pressure, P, a new stable hexagonal (h) crystal structure appears. In this phase regime the chains in the crystals become extended, or at any rate they tend towards chain extension. In addition to these long established facts, we identified unrestrained "thickening growth" in *isolated* crystals where the crystals keep growing continuously in the thickness directions, not only until full chain extension but also beyond, while in the h-phase [3, 4]. This, concurrently with lateral growth, then leads to wedge-shaped crystals (this is the reason for giving attention to the wedge shape). All the above take place in the h-phase only. However, the h-phase (as first described by Bassett and Turner [6, 7]) is not confined to the h-stability regime but arises also in the o-stability regime where the h-phase is thus metastable; in this case the h-crystals may transform to the stable o-crystals at a certain stage of growth. We find that, at least within the P- and T-regimes explored in [1–4], all crystallization takes place in the h-phase; thus the h-phase is a prerequisite for crystallization (hence the role and significance of "true" metastability). Within the o-stability regime, at a certain stage of growth (both thickening and lateral growth), the metastable h-phase transforms into the stable o-phase, when as we have observed, all growth (that is, thickening and lateral) stops or slows down drastically. The latter therefore means that the crystal thickness becomes locked in by the h → o transformation, which is a new, hitherto unsuspected origin of limited lamellar thickness. This lamellar thickness, here resulting from arrested thickening growth, has its own thermodynamic stability criteria both for the h- and o-crystal structures, (hence the significance of size dependence). It is implied further by all the above that the chains in the h-phase are mobile, allowing lamellar thickening from the folded configuration, and, in general, thickening growth as a principal growth mechanism. This forms the basis of a theoretical approach by one of us (MH) [8, 9]. All the above makes the mobile h-phase of special significance in polymer crystallization.

2. Free-energy considerations

To evolve the concept of phase-size-induced stability inversion in phase diagrams we shall resort to the scheme used by one of us elsewhere (in cooperation with Ungar and Percec [10–12]). There it was used to visualize the stability conditions of the liquid-crystalline state, but it could be regarded as more general, being applicable to any state, with a stability intermediate between the stablest crystal (C) and liquid (L), as referred to infinite size, this intermediate state being denoted as M (mesophase) in what follows. Subscripts C, L, M attached to other symbols to be used will refer to the respective phases.

As in [10–12], we start with a schematic free-energy, G, versus temperature plot for a system capable of displaying the C-, M- and L-phases. (Figs 1, 2 and 3). As before, we adopt the gross simplications of taking the G versus T lines as straight and without a change in direction on intersection; this, however, should not affect the validity of the arguments. We start with the situation where the M-phase is unstable; that is, G_M is higher than either G_C or G_L over the entire temperature range. Fig. 1 illustrates such a case. Here the appropriate intersections define the corresponding melting and transition temperatures, $(T_m^\circ)_C$, $(T_m^\circ)_M$ and T_{tr}°. These temperatures correspond to a transformation between two stable phases, $(T_m^\circ)_C$, between a stable and metastable phase, $(T_m^\circ)_M$, in the temperature range concerned, while T_{tr}° is altogether unrealizable (virtual). The symbol $^\circ$ denotes infinite size throughout.

It will be clear that to realize M as a stable phase the relative positions G will need to be changed so as to bring at least one portion of the G_M curve below both G_C and G_L. Following the argument in [10–12] such an "uncovering" of the M-phase can be most conveniently visualized in physical terms by taking two extreme cases, namely, where the principal change is that in G_L, or alternatively that in G_C, with the smaller changes in G_M disregarded in both cases. As seen from Figs 2 and 3, the M-phase can be uncovered if either G_L (Fig. 2) or G_C (Fig. 3) is raised. (For simplicity, this is done solely by displacement with an unaltered gradient. Strictly, this cannot be correct yet, since over a limited T-range and at temperatures far above 0 K the mean vertical displacements will hardly be affected by inclusion of a change in gradient; such changes will be disregarded).

In both cases, Fig. 2 and Fig. 3, the intersections of the various G are marked on the T-axis. It is to be noted in the first place that T_{tr}° has now become real, falling below both $(T_m^\circ)_M$ and $(T_m^\circ)_C$; in both cases, this is consistent with the existence of a stable M-phase. There is, however, an important difference between Fig. 2 and Fig. 3. In Fig. 2 the relevant melting and transformation temperatures have moved upwards, while in Fig. 3 they moved downwards along the T-axis in comparison to their positions in Fig. 1. In other words, the two procedures of uncovering the metastable phase in Fig. 2 and Fig. 3 lead to respective elevation and depression of the relevant melting and transition temperatures.

As broad guidelines we may attach the following

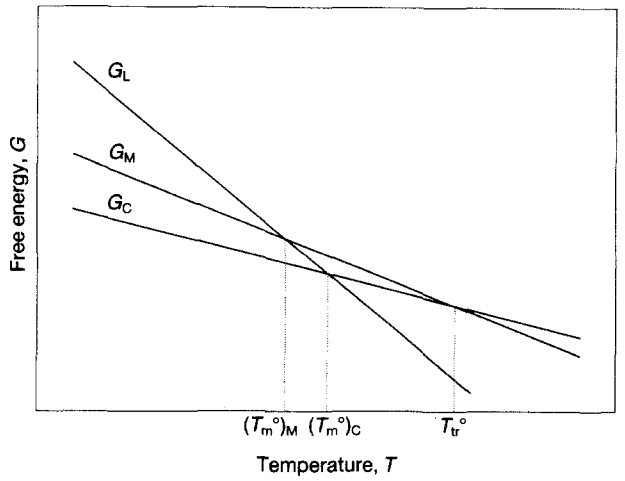

Figure 1 Schematic free energy versus temperature plot illustrating the situation where M-phase is metastable over the whole temperature range.

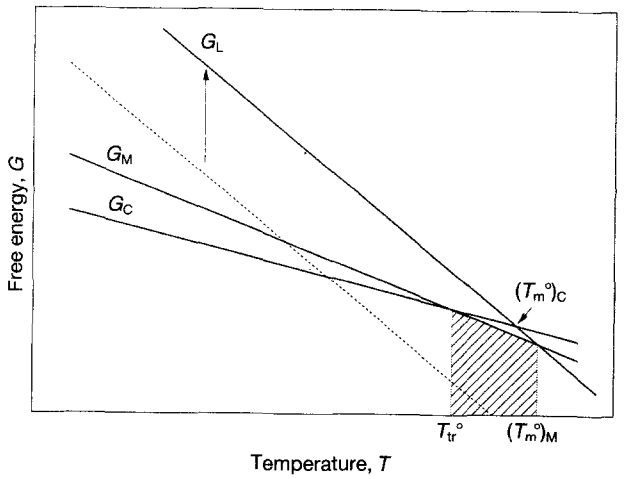

Figure 2 Schematic free energy versus temperature plot illustrating the situation where M-phase has a stable region achieved by raising the melt free energy, G_L.

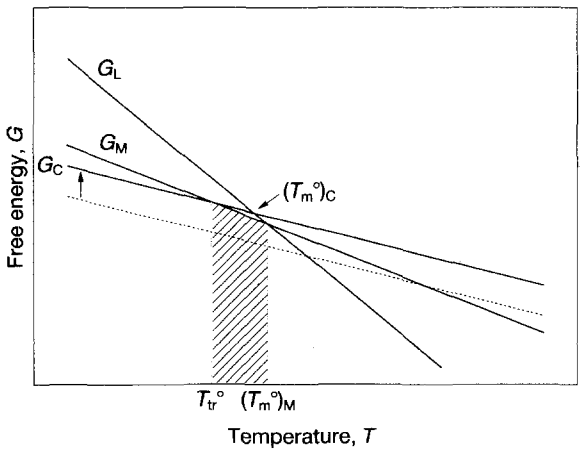

Figure 3 Free energy versus temperature plot illustrating the situation where M-phase has a stable temperature region achieved by raising the crystal free energy, G_C.

physical meaning to situations corresponding to Figs 2 and 3. The raising of G_L in Fig. 2 implies either the raising of H (the enthalpy) or of the lowering of S (the entropy), or a combination of both. Application of pressure will have such an effect, and in most (even if not all) cases this influence is to a much greater extent on the L- than on the C-phases (or the M-phase). The raising of the crystal melting points, with the resulting uncovering of the M-phase, in our case for PE, and the whole subject of pressure-induced crystallization in polymers in general, is the direct consequence of such a raising of G_L (see also [13]). Further, there are a number of other ways in which the entropy of the melt may be specifically reduced, leading to a situation as that in Fig. 2, such as stiffening of the chain by physical or chemical means. The introduction of mesogenic groups and the resulting promotion of a liquid-crystal phase is a familiar example of the latter. Orienting the melt phase, or preventing disorientation on melting of an oriented solid through externally applied constraints, will have an effect in the same direction; this is documented by numerous examples in [10]. When a situation, such as in Fig. 1, applies to the monomeric state, an increase in chain length on polymerization can provoke a change-over to a situation such as that shown in Fig. 2, and hence it can lead to liquid crystals (the polymer effect, see [11]).

The situation embodied by Fig. 3 corresponds to the impairing of crystal perfection. Again, this can arise through physical or chemical means; chemical imperfections in an otherwise regular chain giving rise to lattice defects is an example of a chemical influence. This is consistent with the general experience that less perfectly and/or less readily crystallizable substances are more prone to give rise to mesophases, and liquid crystals in particular; this theme is enlarged in [10]. The raising of G_C, however, will arise not only through impaired lattice order but also through an increase in specific surface of the otherwise perfectly ordered crystal, that is through reduction in crystal size. This particular point will be the centre piece of the argument in what follows.

3. Size-dependent phase stability

3.1. Graphical representation

That size affects the stability of phases is of course well-known. It manifests itself by depression of the pertinent phase-transition temperatures. Our present addition to this subject is the extension to systems which can have various polymorphs (only one of which can be stable at a particular temperature except for the phase line itself); and we draw attention to the fact that, in general, the size dependence of the phase transition will be different for the different polymorphs, which can, in turn, have conspicuous consequences. It is to such situations that we shall draw attention in this paper.

For the purpose stated, we take the G versus T diagram as our starting point and consider the situation shown in Fig. 1, where the M-phase is metastable (the solid lines in Fig. 4). According to the preceding considerations, by decreasing the crystal size, l, we are raising G_C (dashed lines) in two successive stages, l_1 and l_2 (at this stage the size parameter, l, is quite general, later we shall identify it with the lamellar

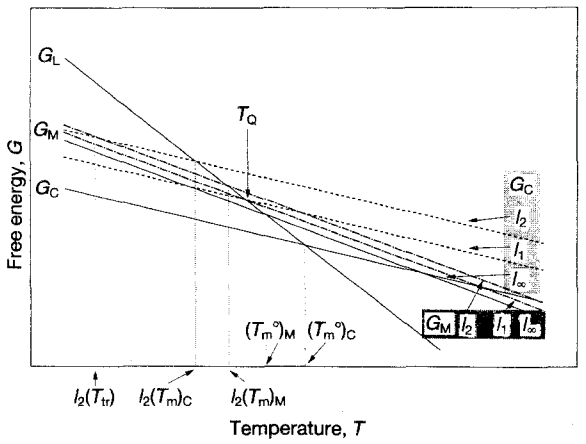

Figure 4 A schematic free energy, G versus temperature, T, plot (as in Fig. 3), for two successive stages of raising G_C, (and G_M). The elevation of G_C corresponds to a successive decrease in the crystal size, l, from l_∞ to l_2 where $l_\infty > l_1 > l_2$. This rise in G, here associated with a decreasing crystal size, is taken to be much smaller for G_M than for G_C, with a consequent crossing over of the relative stabilities of the C- and M-phases with size, (as drawn, for size $l_1 \equiv l_Q$ at the temperature T_Q). For the still smaller size l_2, there is a finite temperature interval $[l_2(T_m)_M - l_2(T_{tr})]$ where the M-phase is the stable phase.

thickness of a polymer crystal). We note that the intersections with G_L shift to successively lower T (that is, eventually to l_2 $(T_m)_C$ in Fig. 4); in other words, the melting point becomes successively more depressed. The same will apply to the M-phase. Here, however, we consider the situation that the effect of size on G_M is smaller than on G_C; that is G_M is being raised by smaller increments for identical size reductions. This, as seen in Fig. 4, has the consequence that, at a certain reduced l-value, G_C "overtakes" G_M, hence the M-phase becomes stable. In terms of T_m this means that $(T_m)_C$ decreases faster than $(T_m)_M$ with decreasing l, so that at a specific $l \equiv l_Q$ one has $(T_m)_C = (T_m)_M = T_{tr}$, where now T_{tr} is real, and at $l < l_Q$ one has $(T_m)_C < (T_m)_M$; that is, the M-phase becomes stable.

The above situation is best represented by plotting the various intersections along the T-axis in Fig. 4 against $1/l$. This is shown by Fig. 5 displaying $(T_m)_C$ (solid line), $(T_m)_M$ (dashed line) and T_{tr} (dotted line), which can be considered as a temperature–size phase-stability diagram. (Here the designation *phase-stability diagram* is adopted so that the term *phase diagram* can be reserved for infinite phases as is usual in thermodynamics). The heavy lines define the stable phase boundaries in the $(T, 1/l)$-plane, i.e. they define the equilibrium phase-stability diagram. The regions with the different hatchings define the phase regimes C and M. Each can be present in a stable and in a metastable form; the corresponding regions can be identified by the key in Fig. 5. The principal message of this phase-stability diagram is that the M-phase, metastable for infinite size, can be the stable phase when l is sufficiently small; the region of stability is defined in Fig. 5. Other features to note are the existence of a triple point, Q, where all three phases (L, C and M) can coexist, and the limits of metastability of each of the solid phases, C and M. Of special

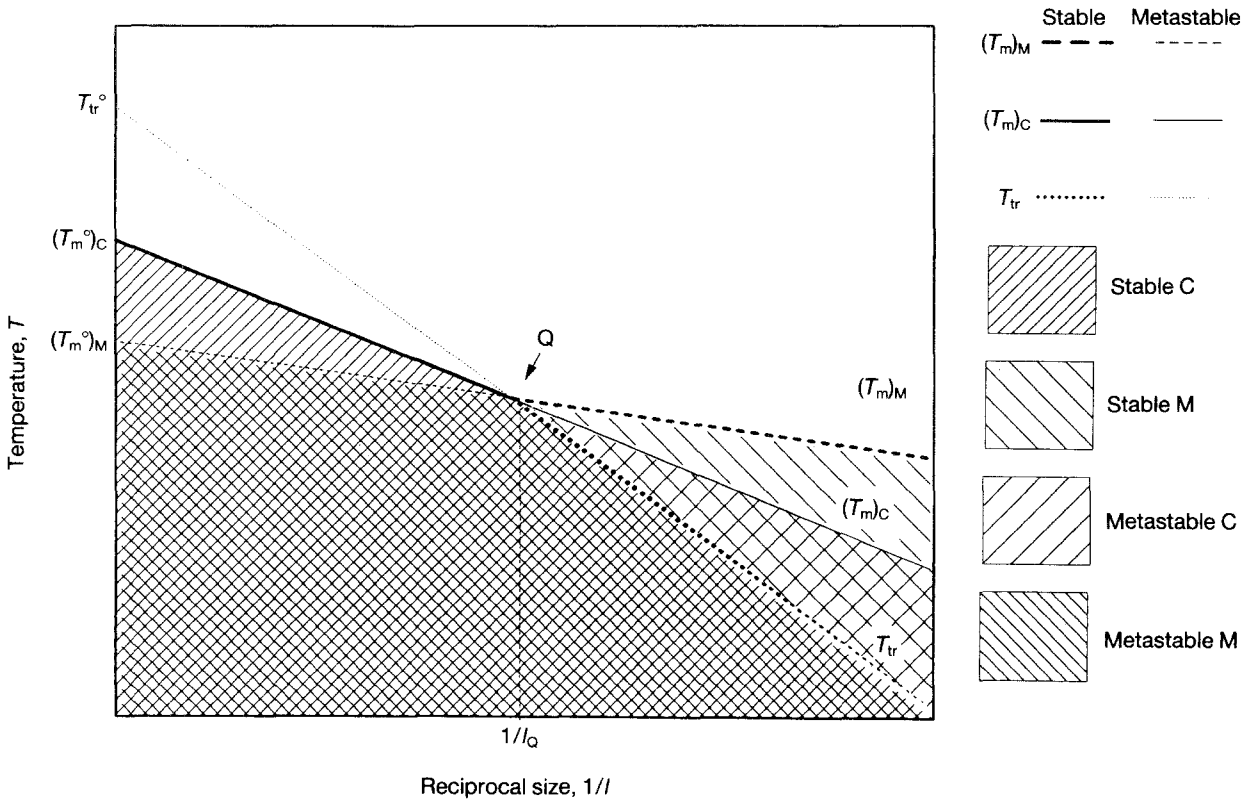

Figure 5 Temperature, T versus reciprocal size, $1/l$, phase-stability diagram obtained by plotting the temperatures of intersection of G in a free energy versus size construction (such as in Fig. 4) displaying the crossing over of the phase stability with decreasing size. (——) C-phase melting, (– – –) M-phase melting, (· · ·) C → M transformation. The intersection of the phase lines defines a triple point, Q, where all three phases (L, C and M) can co-exist as stable phases. The different hatchings, heavy for stable, light for metastable, denote the phase regimes where the C- and M-phases can exist either as stable or as metastable phases.

interest is the situation $1/l = 0$ (that is, infinite phase size), where the M-phase is metastable throughout up to $(T_m^\circ)_M$; beyond this temperature it cannot exist even in a metastable state. This leads to a temperature interval, $(T_m^\circ)_C$–$(T_m^\circ)_M$, where the C-phase alone is possible; for $1/l > 0$ this "C alone" zone gradually narrows down to the triple point. Finally, T_{tr} is virtual for all sizes larger than l_Q.

3.2. Analytical representation

The conditions in Fig. 5 can be readily expressed analytically. The dependence of the phase-transition temperature, T_x (where x specifies the type of transition), on the size of the phase is given by the Gibbs-Thompson relation

$$T_X = T_X^\circ\left(1 - \frac{V_X(\sigma)_X}{l(\Delta H)_X}\right) \tag{1}$$

Where T_X° denotes the infinite phase size, ΔH is the heat of the phase transformation (per unit mass), σ is the mean surface free energy, V_X the specific volume and l is again the dimension of the phase (as characterized by a single parameter). Writing Equation 1 specifically for the phase changes of our concern

$$\begin{aligned}(T_m)_C &= (T_m^\circ)_C\left(1 - \frac{V_c(\sigma)_C}{l(\Delta H)_C}\right)\\ (T_m)_M &= (T_m^\circ)_M\left(1 - \frac{V_M(\sigma)_M}{l(\Delta H)_M}\right)\\ T_{tr} &= T_{tr}^\circ\left(1 - \frac{V_{C-M}\sigma_{C-M}}{l(\Delta H)_{tr}}\right)\end{aligned} \tag{2}$$

where the meaning of the symbols is self-explanatory (σ_{C-M} and V_{C-M} denote the respective differences in the surface free energies and specific volumes between the C- and M-phases). Equation 2 expresses the depressions of the three transformation temperatures due to a decreasing phase size.

It will be apparent that the gradients of the three lines in Fig. 5 are given by the respective values of $V\sigma/\Delta H$. It follows that the precondition for an intersection of the lines, and hence for a triple point, is

$$\frac{V_M\sigma_M}{(\Delta H)_M} < \frac{V_c\sigma_C}{(\Delta H)_C} \tag{3}$$

which, accordingly, is the condition for an inversion of phase stability with phase size, which is, in turn, one of the central themes in this paper.

3.3. Modes of crystal growth

In what follows we shall assume that the inequality in Equation 3, (hence the phase-stability conditions, such as those in Fig. 5)[1] hold (for a discussion see later) and consider the implications for the growth of a new phase. While in principle pertinent to any phase transformation, we shall refer specifically to crystal growth with the solid (crystal) phase capable of having variants C and M.

In Fig. 6 the stable-phase lines (heavy lines in Fig. 5) are denoted by heavy solid lines with the metastable-phase lines denoted by light dashed lines and consider that crystallization is proceeding isothermally. As any new crystal phase will have to start from the smallest possible size, and then proceed to increase in size, the growth pathway at any given temperature of crystallization, T_c, will be along horizontal arrows such as those in Fig. 6. In the L-phase region any crystal that may appear would only be a transient fluctuation ($\leftarrow$ L) until a stable liquid–solid phase line is reached. This will occur when l reaches the size of the pertinent critical nucleus, l^*, beyond which the crystal will be able to grow as a stable phase.

It can be seen from Fig. 6 that there are two regions of T_c above (A) or below (B) the triple-point temperature, T_Q.

(A) $T_c > T_Q$. Here the crystal can, or needs to, appear and grow directly into the crystal phase of ultimate stability ($\leftarrow C_A$). Region A is divided into two zones. A_1 comprises the temperature region $(T_m^\circ)_C$–$(T_m^\circ)_M$. Here the M-phase cannot exist at all. Growth, if it occurs ($\leftarrow C_A$), will necessarily be in the C-phase only. A_2 comprises the temperature region $(T_m)_M$–T_Q. Here, the stable end state is still the C-phase, yet growth may pass through the M-phase, which for all l remains metastable. While this subdivision of A into A_1 and A_2 is significant in principle from the point of view of thermodynamics, it has only a limited effect on the phase transformation itself (see Section 7). Consequently, we shall not emphasize this further here.

(B) $T_C < T_Q$. Here crystals will *need* to pass through the M-phase first, a phase which will be the most stable one for small sizes, specifically when $l < l_Q$. Following $\leftarrow L_B$, l exceeds the critical nucleus at l_M^*. The M-crystal will then grow in the M-phase ($\leftarrow$ M) until the M–C transition line is reached corresponding to l_{tr}^*. Beyond that, growth will continue in the C-stability region ($\leftarrow C_B$) during which an M $\rightarrow$ C transformation may occur. Note that the critical stable nucleus size for the C-phase, $(l_{C_B}^*)$ is reached before that stage, but the corresponding C-phase will be metastable (that is stable with respect to L but unstable with respect to M). Within the whole T range over B we can have two situations. (1) The growing crystal passing through the M–C stability divide (along $\leftarrow C_B$) remains untransformed, and the final product remains in the M-form. In this case we have a metastable end state which can thus be clearly registered as such. (2) The growing crystal does transform into the stable C-form. In this case the final product will reveal nothing of its past history, in particular, whether or not it has passed through a different phase during its growth; the size dependent aspect of its phase history

[1] Fig. 5 uses the three relations in Equation 2 independently. For a rigorous treatment the system would need to be considered as consisting of three components in fact is done for the triple point in Appendix I. The approximation in Fig. 5 would not affect the trends in the present scheme.

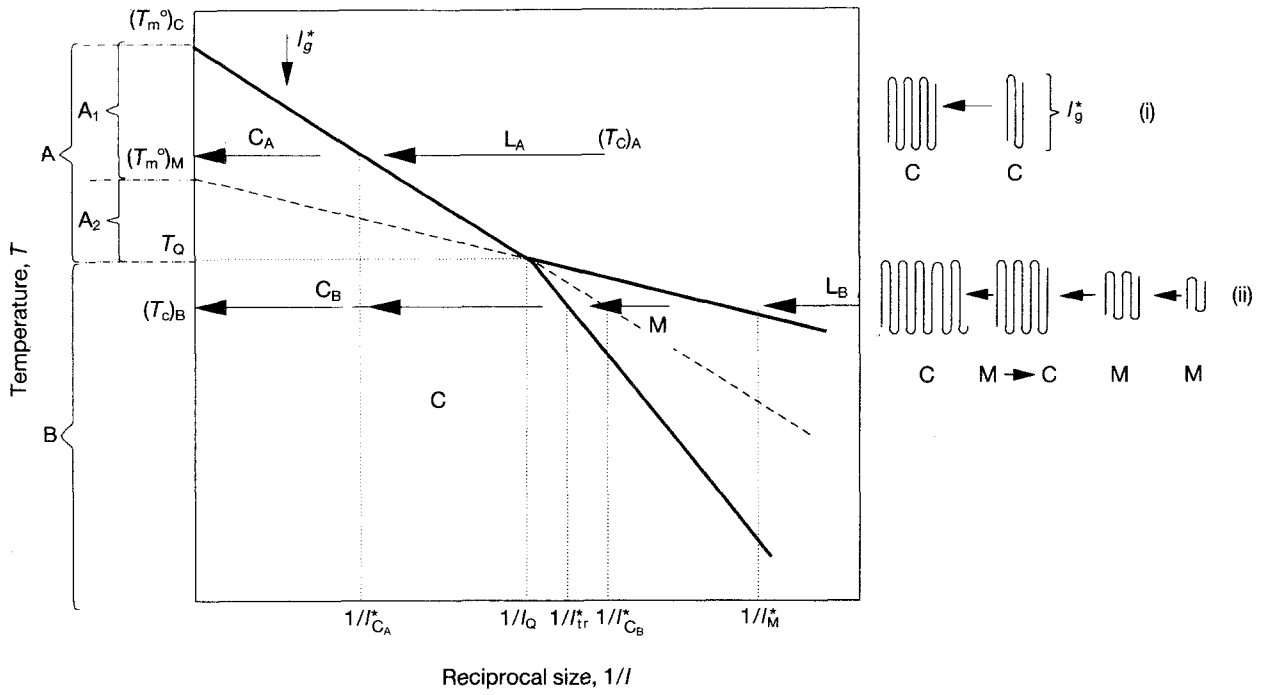

Figure 6 Phase (crystal) growth as a temperature, T, versus reciprocal size, $1/l$, phase-stability diagram, as in Fig. 5. (——) Stable-phase demarcation lines, (– – –) metastable-phase demarcation lines. (→) Pointing towards $1/l_\infty$ denotes isothermal-growth pathways at the selected (crystallization) temperatures, T_c. Two such pathways are indicated, one above and one below the triple-point temperature, T_Q ($(T_c)_A$ and $(T_c)_B$ which are representative of the growth regimes A and B, respectively). l^* refers to the sizes of limiting stability (critical nuclei) of the respective phases. Schematic molecular illustration are given of growth pathways for chain-folded polymer crystallization in (i) regime A, and (ii) regime B. Here (i) corresponds to the traditionally envisaged mode of growth, which is exclusively lateral at a fixed, kinetically determined thickness l_g^*, where $l_g^* > l_{C_A}^*$, but it is now confined to region A; (ii) corresponds to simultaneous growth both in the lateral and the thickness directions (thickening growth), the latter is terminated by the C → M transformation somewhere along the arrow C_B in the C stability regime. The necessity of this mode arises in the newly recognized region B.

is thus obliterated. Nevertheless, even in this case, the *phase history* should still be reflected by the kinetics of the growth process if followed during the initial stages of growth. This issue, to our knowledge has never been addressed; we shall return to it later with reference to polymer crystals.

The above argument is based purely on thermodynamics. Whether both modes A and B will occur in the same system will depend on additional kinetic factors. Thus, if the interval $(T_m^\circ)_C$–$(T_m^\circ)_M$ is narrow, then T_C will be confined to low supercoolings for crystallization by mode A, where crystallization may be too slow for this mode-A to appear in practice. Alternatively, if the $(T_m^\circ)_C$–$(T_m^\circ)_M$ interval is very wide then mode-B can only take over at a value of T_C corresponding to high supercoolings. As the system will always need to be cooled from a T-value lying above $(T_m^\circ)_C$ to T_c, in this latter case crystallization in mode A may well set in along the long cooling pathway before the intended T_c is reached, in which case mode B would not be attainable in practice. This distinction, namely, whether only A or only B is realizable in practice, could be an important divide between materials, and so far to our knowledge has remained unenunciated.

4. Application to chain-folded polymer crystallization

The above considerations can be readily transferred to the situation of chain-folded lamellar crystal growth. Accordingly, Equation 2 will read

$$
\begin{aligned}
(T_m)_C &= (T_m^\circ)_C\left(1-\frac{2(\sigma_e)_C}{l(\Delta H)_C}\right)\\
(T_m)_M &= (T_m^\circ)_M\left(1-\frac{2(\sigma_e)_M}{l(\Delta H)_M}\right)\\
T_{tr} &= T_{tr}^\circ\left(1-\frac{2(\sigma_e)_{C-M}}{l(\Delta H)_{tr}}\right) \qquad (4)
\end{aligned}
$$

where l denotes the lamellar thickness, σ_e denotes the surface free energy of the basal planes (fold surfaces). Equation 3 thus acquires the form given by Hoffman and Weeks for the melting points [14][2].

Here the special polymeric feature is constituted by the fact that the limiting phase size is the lamellar thickness and the relevant growth direction is the process of lamellar thickening growth when it occurs, (see [2–4]). Of course the lamellae also grow laterally [1, 2], but here the dimensional range where the size has any effect on the phase stability is soon exceeded,

[2] Although not usually pointed out, passing from Equation 2 to Equation 4 implies the following changes in the definition of the symbols and in the restrictions. (*i*) ΔH here refers to a unit volume of the transforming phase. (ii) This allows for differences in specific volumes of the alternative phases, hence the absence of the V terms in Equation 4. (iii) Volume changes are only due to changes in l; (iv) There is no difference in the amount of material along l in the alternative phases (this arises from the fact that the chains are straight in both the alternative phases with only negligible length differences).

leaving the lamellar thickness as the dimension determining the phase stability. Traditionally, polymer crystallization is envisaged as being confined within range A, (ignoring at this point the subdivision into A_1 and A_2, see Section 7); this is treated by the extensive literature on polymer crystallization. As seen, this is only a small portion of all possible crystal-growth modes, the totality of which include growth pathways via an M-phase in range B. The introduction of mode B is new, and it has been prompted by the experimental observations in [1–4]. To give this widened scope explicit meaning we need to specify the nature of the M-phase first.

At this point we can link up with the extensive past works on PE in general, and with our preceding papers [1–4] in particular. Namely, we know that PE can have a phase, the hexagonal (h) phase, which is intermediate between the commonly stable orthorhombic (o) phase and the liquid melt (L) [6, 7]. As is well known, this mesomorphic h-phase is realizable as a stable phase under pressure (shown schematically in Fig. 7) where the chains are highly mobile, so that they can refold readily towards full chain extension – from an initially highly folded conformation in the course of crystal growth – which is the commonly perceived source of the extended-chain-type crystal morphology [15, 16]. As a consequence of the above, studied extensively in [1–4], an isolated crystal lamella, when in the h-phase, grows simultaneously in the lateral and thickness directions (the newly defined thickening growth); this is in contrast to the conventionally envisaged lamellar growth, where the lamellae grow only laterally with unaltered crystal thicknesses (except for some slow or belated lamellar thickening – a secondary crystallization process referred to in the past as isothermal thickening). All the above knowledge of the h-phase was gained in experiments at elevated pressure. Without some special measures (see, for example, [10]) the h-phase is normally unrealizable at atmospheric pressures, since it is metastable with free-energy relations as in Fig. 1.

In view of the above, the phase relations in Fig. 5 could conceivably apply at atmospheric pressure, provided the inequality in Equation 3 holds when applied to the PE system. Namely

$$\frac{(\sigma_e)_h}{(\Delta H)_h} < \frac{(\sigma_e)_o}{(\Delta H)_o} \tag{5}$$

This would mean that, for a sufficiently small size, l, the h-phase would be the thermodynamically stable phase, creating a stable h-regime in the T–$1/l$ phase-stability diagram.

The above would further imply the applicability of the crystal-growth scheme in Fig. 6. Accordingly, we would have modes A and B. Mode A would be as traditionally conceived, (Fig. 6i), namely, crystals nucleate and grow in the o-phase throughout. This would occur with a constant thickness, l_g^*, as denoted by the present models of chain-folded crystal growth where $l_g^* > l_o^*$, the critical nucleus length for the o-phase (with $l_g^* - l_o^*$ small, see Fig. 6i). In contrast, mode B brings in new considerations as schematically indicated by Fig. 6ii. Accordingly, the crystal starts life in the h-phase with rapid thickening growth, as along ← M in Fig. 6ii, to follow. On traversing the stable h–o boundary, which in Fig. 6 would correspond to the M–C boundary, the h-phase could transform into the new stable o-phase. From previous experiments [1–4], at this stage of transformation (somewhere along ← C_B in Fig. 6) thickening growth would stop (or slow down drastically), thus *locking in* the lamellar thickness appropriate to the stage of thickening growth where this transformation takes place. Thus mode B, as applied to the chain-folded crystallization of polymers, with appropriately mobile intermediate phases, would provide a new, previously unrecognized source for the finite lamellar thickness, which is the principal characteristic of polymer crystals.

5. Combining pressure and size dependence: a unified presentation of possible crystal-growth paths

In region B in Fig. 6, we placed a new growth mechanism for chain-folded crystals on the map; this arose from the combination of the new thermodynamic considerations with sliding diffusion in the mobile phase, where the mobile phase may only possess a transient size-determined stability. We shall now proceed to place this potential mode of crystal growth in the context of other possible growth pathways, such as would arise from a complete (P, T, $1/l$) phase diagram, and this will be linked, wherever possible, with known experience.

Fig. 7 is a schematic representation of a (P, T)-phase diagram for a crystal of infinite size which should be familiar from traditional studies of crystallization under pressure [6, 7, 13, 16]. It displays the well-established h-phase regime beyond the triple point, which is our source of knowledge of the mesophase on which the present argument is based. We shall assume that this is the same h-phase which was invoked in Fig. 6, resulting from the limited crystal

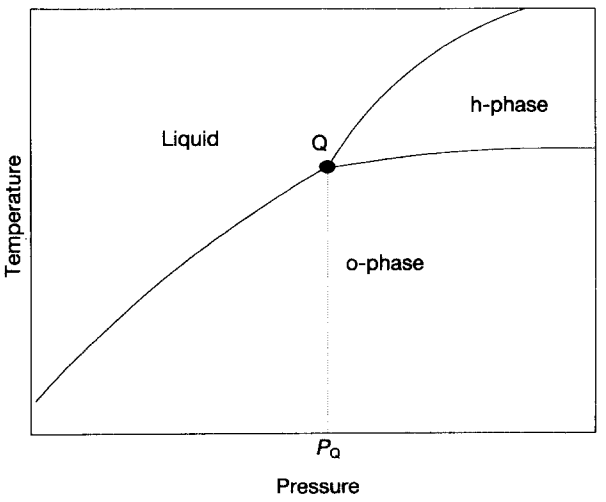

Figure 7 A temperature–pressure, T–P, phase diagram (referred to infinite phase size) of the kind observed for PE [16] displaying orthorhombic (o) and hexagonal (h) crystal phases (corresponding to C and M respectively in Figs 1–3). Beyond P_Q (the triple point) there is a stable hexagonal regime even for infinite phase size.

size, in which case there should be continuity between the h-phase regimes in Figs 6 and 7. This is demonstrated by the full (P, T, $1/l$) phase-stability diagram drawn schematically in Fig. 8. This shows a continuous region of stable h-phase extending from the previously considered high P to 0 pressure (that is, atmospheric pressure) but for correspondingly reduced crystal sizes. The two individual triple points in Figs 5 and 7 now become connected forming a *triple line*, which can be calculated analytically from parameters defining the two extreme cases in Figs 5 and 7 (see Appendix I). As will be seen from Appendix I, this analytical expression, in addition to defining the triple-line itself, reveals a singularity in terms of the input parameters. This was totally unsuspected, and it promises to be of wider significance for phase considerations, particularly where differences between specific volumes are small; this is an issue calling for separate attention.

Having introduced the full (P, T, $1/l$)-phase-stability diagram we can now proceed to consider the different growth pathways. In this we maintain isothermal and isobaric conditions and consider the effect of increasing l. For this we take (T, $1/l$)-sections, of the (P, T, $1/l$)- phase-stability diagram at appropriately chosen constant P and we follow crystal growth at chosen values of constant T within these sections. We take the following cases.

1. $P > P_Q$, that is, above the triple point. Here we have a stable h-regime for infinite crystal size. The corresponding (T, $1/l$)-section is shown in Fig. 9. When the inequality in Equation 5 holds, growth will always pass through the h-phase, but according to the choice of T_c we have two regimes. When $T_c > T^\circ_{tr}$, the crystal will stay in the h-regime throughout ($\leftarrow$ 1). Since the h-phase is mobile, there will be continuous thickening growth during the full life span of the crystal (unless, of course, it is arrested by mutual impingement of the crystals [2]). This is the mode which corresponds to the well-established extended-chain-type crystallization [15, 16]. For $T^\circ_{cr} < T^\circ_{tr}$ ($\leftarrow$ 2) there will be a h $\rightarrow$ o transformation after the growing (thickening) crystal crosses the T_{tr} line. Hence, the situation will be qualitatively the same as in mode B in Fig. 6. Again, we have observed this mode under the conditions in Fig. 9, (that is at elevated P) experimentally [2].

2. Next we take a (T, $1/l$)-section at $P < P_Q$, that is below the triple point. For this situation, considerations in Fig. 6 pertain; that is, we should have two modes, A and B. In this respect all sections for $P < P_Q$ are the same; the only difference is that the region A widens (in terms of T) when going to lower P. Nevertheless, as pointed out previously, this widening of A can in principle have a profound effect on the growth path actually observed due to kinetic reasons. Namely, when the A-interval is very narrow, mode A may be too slow to become observable; and when it is very wide, mode B may not be reached. In what follows we shall consider these two situations (namely a narrow and wide region A, in terms of T) separately; this is a readily visualizable variant of Fig. 6.

First, consider the situation of a (T, $1/l$)-section for large P (in the region below P_Q, that is, for P not much

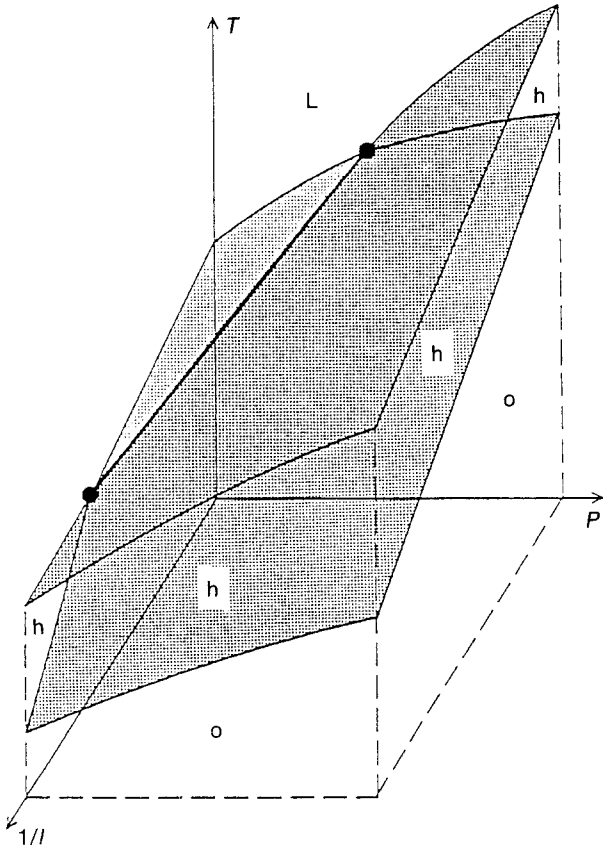

Figure 8 Combined three-dimensional temperature–pressure–reciprocal size (T, P, $1/l$) phase-stability diagram for a situation when Figs 5, 6 and 7 would apply separately. The notation, is potentially applicable to polyethylene (that is, C and M in Fig. 5 correspond here to o and h). The continuous shaded region (a volume in three-dimensional space) is a region where the intermediate phase (here h) is stable, connecting the corresponding region in Fig. 7 (infinite size) with those in Figs 5 and 6 (finite size). The triple points become the extremities of a new *triple line*, (see also Appendix I) which defines the boundary below which the h-phase can (or cannot) exist.

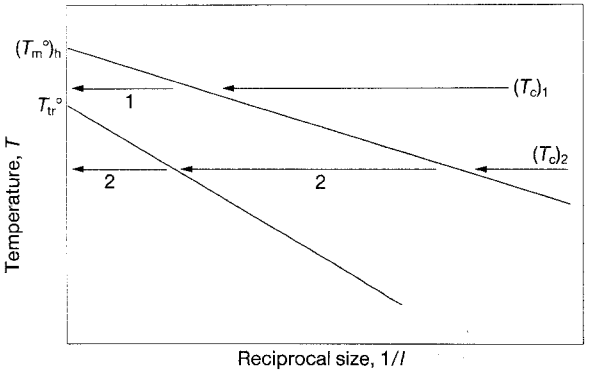

Figure 9 A ($1/l$) section of the phase-stability diagram in Fig. 8 for a constant P with $P > P_Q$. There is now a stable h-region for all l. $\leftarrow(T_c)_1$ and $\leftarrow(T_c)_2$ define two isothermal-growth pathways at two-different temperatures. Along $(T_c)_1$, the h-phase is stable up to $l = \infty$; here, the growth mechanism leading to extended chains (and beyond – unlimited thickening growth) applies, as in the first 2 stages of (ii) in Figure 6). Along $(T_c)_2$, the situation becomes as in mode B of Fig. 6; that is, it leads to a h $\rightarrow$ o transformation and cessation of thickening growth with C $\equiv$ o and M $\equiv$ h).

below P_Q), where the interval A exists but is small. This is the situation in much of the experimental work in our own preceding papers [1–4, 17]. It was observed that there was a narrow non-growth region $(T_m^\circ)_o$–$(T_m^\circ)_h$, with growth only setting in for T_c below this region, when it was exclusively in the h-phase; The growth stopped (or drastically slowed down) on the h → o transformation[3]. This is clearly consistent with the situation anticipated kinetically from a narrow A-interval where crystallization in mode A remains unachievable with all the observable crystallization taking place in mode B.

The second extreme situation, that of a very wide region A, connects with the question of overriding importance as to what happens as P is lowered. Specifically, how wide should interval A be for mode A (that is direct crystallization in the o-phase) to set in? And further, how far should mode B be depressed for it to become inaccessible? Or more specifically, what is the situation at atmospheric pressure to which most of available experimental material pertains forming the basis of existing crystallization theories? Looked at it in this way, the different existing models for crystallization, and the newly proposed model involving the mobile transient h-phase, need not conflict in principle; they would be valid in different regimes of the (P, T, $1/l$)-phase-stability diagram. The regimes themselves are thermodynamically defined, hence they lie on a solid foundation. The question which needs assessing is whether the corresponding growth pathway is kinetically realizable, or not, under the given circumstances.

In Section 9 we shall probe quantitatively the feasability of crystal growth in mode B for PE under atmospheric conditions. Specifically, can it occur at all and at what T_c? For this purpose we recall that $(T_m^\circ)_o$ for PE is held to be 145 °C and the upper limit of observable crystallization in practice is 130–131 °C. The questions which arise are as follows. Is the gap 145–131 °C an extension of the non-growth region in [1–4]?; that is, does it correspond to region A in Fig. 6 (see also Footnote 3). If so, the absence of crystallization could be associated with the unattainability of the h-phase in that region, which in turn would imply mode-B crystallization at all T_c, when crystallization does takes place, with all that this would imply. Alternatively, if crystallization, at 130 °C and below is in mode A (as was implicitly always assumed in the past), is there a lower T_c at which it could change into mode B? For this we would need to assess the value of T_Q at atmospheric pressure. These questions will be addressed in numerical terms in Section 9. It will then be apparent, even by the most conservative expectations, that mode-B crystallization is at least feasible for crystallization from the melt, irrespective of whether this is the exclusive mode or whether it coexists and/or competes with the traditional mode A.

Finally, we may give some thought to crystallization from solution, the mode by which chain-folded lamellar crystallization was first recognized and on which the most abundant and precise information is available. Here we merely present some pointers to this issue, from which it appears that, in the case of solutions, a depression of $(T_m^\circ)_h$ and T_Q, and hence of the B-range, is expected, which then makes growth in mode B by the previous arguments less likely. This is a reassertion of existing expectations, which have so far been taken for granted, that solution-grown crystals have arisen through mode-A growth only. The argument is as follows.

Consider the free-energy diagram in Fig. 1, pertaining to PE as a single-component system of infinite size. When passing to solutions, the entropy of mixing (together with any solvent–polymer interaction, if applicable), will *lower* G_L. Hence, in this case, the G_L-line will need to be displaced *downwards*. It will be apparent from Fig. 10 that all intersections along the T-axis will then move downwards (in terms of T); this is consistent with the self-evident fact that the melting point (in this case the dissolution temperature, T_d) will be lower. Further, it is readily seen that not only the absolute T-values will be lowered but the differences will also increase; that is, $(T_d^\circ)_C - (T_d^\circ)_M > (T_m^\circ)_C - (T_m^\circ)_M$. Translating this into (T, $1/l$)-phase-stability diagrams via constructions equivalent to Fig. 4 (not shown), this means that interval A widens, and consequently the B-interval will be depressed. The above assertion follows from this; namely, preferential, or possibly exclusive, dominance of growth in mode A.

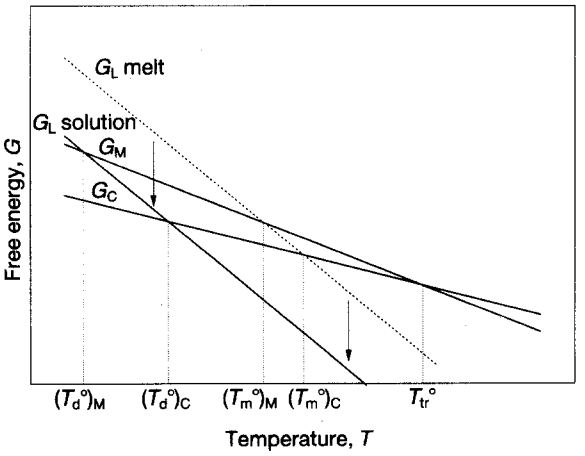

Figure 10 A schematic free-energy–temperature plot (G–T), as in Fig. 2, but showing the effect of lowering (as opposed to raising) of the G_L line. All phase-transition temperatures are lowered with simultaneous widening of the intervals between them, with the initially metastable M-phase remaining metastable and even becoming increasingly metastable. This will be the situation when (in a case such as that shown in Fig. 1, pertaining to a single-component system – solidification of the melt) we pass on to a binary system (a solution) where G_L is lower in the mixed phase (the subscript d denotes dissolution).

[3] This would imply that the non-growth region corresponds to A_1. It follows from what will be said in Section 7, that it should also embrace region A_2 where the h-crystals could exist as a metastable phase but, by the argument in Section 7, they would grow more slowly than the o-crystals. This issue, which requires further experimental attention, will be deferred for the present, where we shall broadly designate the non-growth region by A with no subdivision into A_1 and A_2.

6. Direct evidence of the size dependence of the phase transition in 1–4 poly-*trans*-butadiene

Rastogi and Ungar [18] have demonstrated the reality of a crystal-size-determined phase transition in the case of 1–4 poly-*trans*-butadiene (1–4 PTBD), following some preliminary pointers by Finter and Wegner [19]. Their experiments are of obvious significance for the present discussion, and they can be represented in terms of the presently adopted schematics as follows.

1–4 PTBD has two stable crystal forms even at atmospheric pressure: a monoclinic (m) structure stable at lower temperatures, and a hexagonal (h) structure stable at higher temperatures, with an m → h transformation at around 70°C. Here the m-form is closely analogous to the o-form in PE (except for its lower symmetry) and the h-form has obvious similarities to the PE h-structure. Rastogi and Ungar have shown that the transition temperature is not uniquely defined but depends on the crystal thickness, where a h → m transition can be provoked through isothermal thickening setting in and proceeding while in the h-phase.

The starting samples consisted of solution-grown single crystals sedimented in the form of mats. They were then subjected to heat treatments which activated phase transformations (assessed *in situ* by synchrotron generated X-ray diffraction both at wide and low angles) which are best displayed in terms of a (T, $1/l$)-phase-stability diagram, such as Fig. 11.

Fig. 11 is closely analogous to Fig. 9 except that in the case of 1–4PTBD, it refers to atmospheric pressure. The first step consisted of raising T (↑ 1) to 70 °C (point J). J lies above the m → h transformation point (as commonly conceived). The initial m-structure transforms to a h-structure, which is observed *in situ*. The sample is then held at constant T, corresponding to the point to J, during which rapid thickening (the increase in l, ← 2) is observed by *in-situ*, low-angle X-ray scattering. In the course of this isothermal thickening, a reversed h → m transformation sets in at some stage; that is, the starting phase was again seen.

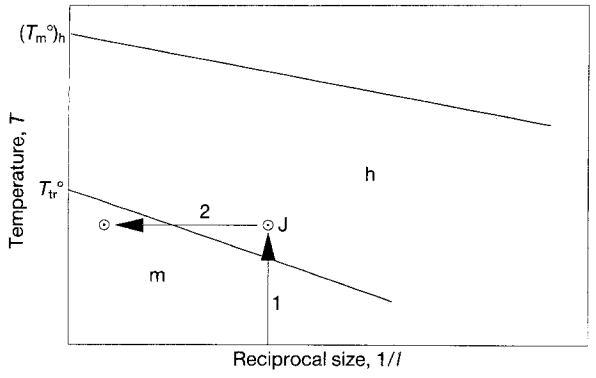

Figure 11 A temperature–size (T–$1/l$) phase-stability diagram such as in Fig. 9, but here relating to the experiments on poly 1–4-*trans* in the present butadiene [18], as expressed by the phase scheme paper. In this case the diagram applied to atmospheric pressure where the h-phase can be stable between T_{tr}° and $(T_m^\circ)_h$. ↑1 and ← 2 denote the pathway adopted in those experiments serving to demonstrate a size-controlled solid–solid phase transition (see text).

This corresponds to ← 2, in Fig. 11, crossing the m–h phase line in the (T, $1/l$)-phase-stability diagram.

The above experiments clearly demonstrate that the h↔m transformation is size (here thickness) induced; this is, to our knowledge, the first demonstration of such an effect in any system. Additionally, it shows that the thickening itself is a consequence of having brought the system into the h-phase in the first place. In the case of a polymer this is mobile, enabling refolding to greater thicknesses, a process which then terminates the life-span of the same h-phase which had brought the thickening into being in the first instance. The thickening could not be followed beyond the h → m transformation stage (the diffraction effects were too close to the primary beam); but from the behaviour just below the m–h phase line, cessation (or drastic slowing down) of the thickening can be reasonably assumed. While these experiments refer to refolding, that is, perfecting of crystals formed already, and not to primary crystal growth itself, they contain several of the essential ingredients of mode-B growth in Fig. 6 (such as a size-dependent phase stability and enhanced thickening in the h-phase, and its consequent self-termination in the m-phase) thus providing support for the reality of such a growth mode. We also note that pressure is not a prerequisite for such a mode of crystallization. It just happens that in the much studied PE system substantial pressures are required if the mobile h-phase is to be observed – a requirement which does not hold for 1–4 PTBD, and possibly several other polymers where the mobile h-phase can exist at ambient pressures (for example, in fluorohydrocarbons).

7. Combined phase-stability and kinetical considerations with a revisit of Ostwald's rule of stages

It will be shown in this present section that the preceding phase-stability considerations can be linked to the kinetics of the phase transformation with potentially important consequences. These considerations include, amongst others, connections with the by now largely forgotten Ostwald's rule of stages [20], providing a combined kinetics- and thermodynamics-based justification, including specification of the limits of validity.

7.1. Phase-stability diagram and critical nucleus

The above stated connections arise from the meaning of the phase-stability diagrams themselves. Namely, the phase lines in the (T, $1/l$)-diagrams represent the minimum size at which a particular phase can be stable at a given T, which is in fact the size of the critical nucleus, l^*. Thus, when crossing a phase line along one of the arrows in Fig. 6 we are in fact traversing the size of the corresponding l^*, hence surpassing the principal activation barrier in the kinetics of crystal (or in general, phase) growth. The connection between the purely thermodynamic considerations implicit in phase-stability diagrams and those of the

kinetics of the phase transformation will therefore be apparent.

It is instructive to plot the critical nucleus size, l^*, itself as a function of T for both the stable and metastable phases (Fig. 12). Although this is just another way of representing the phase-stability diagram (Fig. 6 with *stable* and *meta* replacing C and M respectively, here and throughout Section 7) it serves to bring out the familiar fact that l^* is infinite for the T_m° of the respective phase and that it decreases in inverse proportion to the respective supercooling, ΔT, according to the relation

$$l^* = \gamma \frac{\sigma(T_m^\circ)}{(\Delta H)(\Delta T)} \tag{6}$$

where σ is the mean surface free energy and γ is a constant (see Footnote 5 below). As $(T_m^\circ)_{meta} < (T_m^\circ)_{stable}$ it follows that if $(\sigma/\Delta H)_{meta} < (\sigma/\Delta H)_{stable}$ (note this is the same condition as introduced in Equation 3), then the curves for l^*_{meta} versus T and l^*_{stable} versus T will cross. The cross-over temperature T^* is identical to T_Q identified previously as the triple point in the phase-stability diagram. This mode of presentation explicitly conveys the salient message that, in the case of two or more alternatives, a phase transformation between one equilibrium state to another should commence through the phase variant which has the smallest critical nucleus, l^*. This assertion, itself subject to Equation 3, rests on thermodynamic considerations alone. We shall proceed to show that the same pathway through stages of maximum thermodynamic stability can also correspond to the pathway along which the overall transformation between two ultimately stable phases (that is, of infinite size) can proceed fastest, hence along the one which is also favoured kinetically. The origin of this connection, clearly, rests in the fact that the critical nucleus, defined by the phase lines in the phase-stability diagram, is also the barrier which needs to be surmounted in the course of the kinetics of the phase transformation.

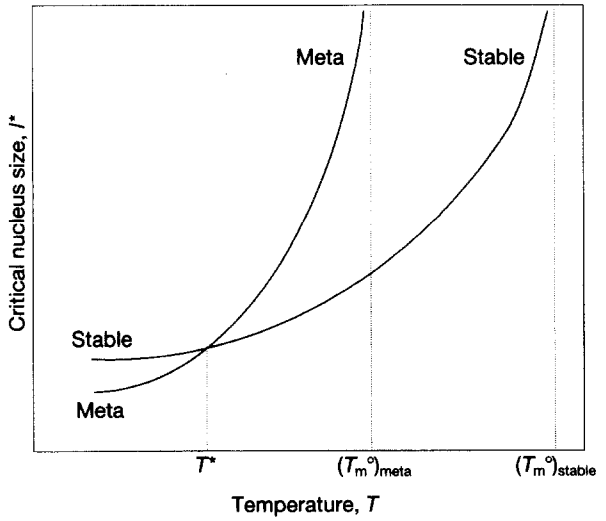

Figure 12 The size of the critical nucleus, l^* as a function of temperature in a system which can form two alternate new phases (for example, polymorphs) of which only one can be stable (hence the other is metastable). For the conditions stated in the text, the curves cross over (T^*). The correspondence between T^* and T^+ (Fig. 13 representing rates) will be apparent, and so will the correspondence of the relevant T intervals to the regions (i), (ii) and (iii) in Fig. 13.

7.2. On rates involving metastable phases

First, we invoke a long-standing experience, namely that in the course of the transformation of one initially stable phase into another, metastable phases (that is, phases of intermediate stability) evolve faster than their corresponding stable versions. (For current examples see Footnote 4). This assertion, while broadly obeyed, has, nevertheless, intrinsic limits to its validity in terms of temperature; we shall return to this point later.

Next, consider the factors determining the overall rate of a phase transformation, R. As should be familiar, R is compounded of the rate at which the new phase nucleates and of the rate at which it grows. When R is compared for two competing phases, it needs first to be considered which of the two processes (namely nucleation or growth) is the rate-determining factor for the overall phase transformation. The following consideration will primarily apply to nucleation. Thus, they will apply to the generation of the new phase (that is, to primary nucleation) unconditionally. They may also apply to the growth stage provided growth is nucleation controlled (secondary nucleation). The latter will be the case for chain-folded-polymer crystal growth, which is generally envisaged as a (secondary) nucleation-controlled process. Consequently, the rate considerations to follow should apply to the crystallization of polymers on both counts, while in the case of other systems and other kinds of phase transformations they should apply only in as far as the nucleation-controlled portion of the overall phase evolution is concerned.

The rate of nucleation, N, is of the form

$$N = \alpha \exp\left[-\frac{\beta}{T(\Delta T)^{n-1}} \right] \tag{7}$$

where the pre-exponential, α, contains transport and frequency terms, and the exponential β relates to the work to form a nucleus of critical size and it is given by

$$\beta = \frac{\sigma^n}{\Delta H^{n-1}} \frac{(T_m^\circ)^{n-1} K}{k} \tag{8}$$

where k is the Boltzmann constant, K contains factors relating to the particular geometry, and the rest of the symbols are as defined previously. The value of n is either 3 or 2, according to whether primary or secondary nucleation is involved.

We proceed by comparing the rates of phase evolution, R, of a stable and metastable phase in the course of a phase transformation on the condition that nucleation is the rate-controlling step. The metastable phase will dominate, that is,

$$R_{meta} > R_{stable} \tag{9a}$$

in the case that

$$N_{meta} > N_{stable} \tag{9b}$$

Equation 9b sets certain requirements on α and β in Equation 7. To have a full picture of when Equation

9b is satisfied, we need to compare R versus T curves for stable and metastable phases for different choices of α and β. Such a mapping is carried out in Appendix II, which should provide an overview, for the first time to our knowledge, of the comparative relation of stable- and metastable-phase development on the basis of Equation 7 for situations when $\alpha_{meta} > \alpha_{stable}$ and $\alpha_{meta} < \alpha_{stable}$, and for both cases, when $\beta_{meta} < \beta_{stable}$ and $\beta_{meta} > \beta_{stable}$. For the present purposes, we shall lift out those cases which we consider most pertinent to the subject of the main body of the paper; the rest are left to Appendix II.

Consider, first, the factor α. Here the transport portion will not greatly differ for the stable- and metastable-phase alternatives, but the frequency term, reflecting the success rate in attachment, should. As there are fewer restrictions for successful attachment in the case of the metastable phase we would expect

$$\alpha_{meta} > \alpha_{stable} \tag{10}$$

Under the conditions expressed by Equation 10, if Equation 9 is to be realised (that is, faster growth in the metastable phase), then the condition

$$\beta_{meta} < \beta_{stable} \tag{11a}$$

needs to be satisfied which, for closely similar values of K and T_m°, will amount to

$$\left(\frac{\sigma}{\Delta H}\right)_{meta} < \left(\frac{\sigma}{\Delta H}\right)_{stable} \tag{11b}$$

This is a necessary but not sufficient condition for the metastable phase to evolve faster. Namely, for Equation 9 to hold, at a given $T < (T_m^\circ)_{meta} < (T_m^\circ)_{stable}$ the effect due to Equation 11a must override the opposing effect due to the ΔT terms. This arises from the fact that, for a given T, it is intrinsic that

$$(\Delta T)_{meta} < (\Delta T)_{stable} \tag{12}$$

In view of the fact that, on decreasing T, the ratio $(\Delta T)_{meta}/(\Delta T)_{stable} \to 1$, while that of $(\sigma/\Delta H)_{meta}/(\sigma/\Delta H)_{stable}$ remains approximately constant, the exponents in N for the two phases will become equal at some value of T sufficiently below $(T_m^\circ)_{meta}$, which defines the temperature, T^+ (see Fig. 13), at which the two rates will cross over, that is, below which the metastable phase becomes dominant. Here T^+ is given by

$$\frac{(\sigma_{meta})^n (T_m^\circ)^{n-1}_{meta}}{(\Delta H)^{n-1}_{meta}(\Delta T_{meta})^{n-1}} = \frac{(\sigma_{stable})^n (T_m^\circ)^{n-1}_{stable}}{(\Delta H)^{(n-1)}_{stable}(\Delta T_{stable})^{n-1}} \tag{13}$$

where $(\Delta T)_{meta} \equiv (T_m^\circ)_{meta} - T^+$ and $(\Delta T)_{stable} \equiv (T_m^\circ)_{stable} - T^+$ with $n = 3$ or 2 according to the nucleation type.

It can be seen that Figs 13 and AII.1 and AII.2 (in Appendix II) display three regions in terms of T: (i) is the exclusive region of the stable phase, (iii) is the region where the metastable phase dominates, and region (ii) is in between, where the two alternative phases compete, (the delineation of the latter is defined, somewhat arbitrarily, by T^+ and $(T_m^\circ)_{meta}$ so as to provide some physically identifiable boundary condition – see below and the caption to Fig. 13).

Curves such as those in Fig. 13 indicate how and why metastable phases can arise in preference to their stable counterparts on the basis of rate considerations alone[4]. True, their dominance by rate will only apply below a certain temperature, T^+, yet it can be readily envisaged how in the usual practical situations, for example, in solidification on rapid cooling, the metastable phase may prevail due to its higher rate at the lower temperature.

Next, we may briefly consider the situation on departing from Equations 10 and 11, which, as will be apparent, are physically less realistic, or even unrealistic. For $\alpha_{meta} < \alpha_{stable}$, with $\beta_{meta} < \beta_{stable}$, there can be two cross-overs, depending on the relative values of α and β (Fig. AII.3, Appendix II). This means that Equation 9 could still apply, but it would have a lower

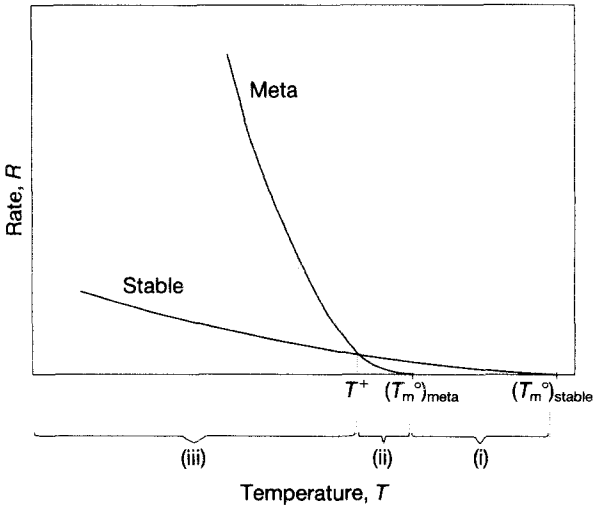

Figure 13 Curves for the rates, R of phase formation as a function of temperature for the case where an alternative (for example, a polymorphic) phase can arise of which only one can be stable (hence the other is metastable), showing the mutual relation of the two rate curves on the same temperature scale. The curves cross over at T^+ defining three T-regions: (i) only one phase, the stable phase, can form, (ii) stable- and metastable-phase formation compete kinetically and (iii) metastable-phase formation dominates (the validity region of Ostwald's rule of stages). This schematic representation reflects a documented real situation observed in a monotropic liquid-crystal-forming system [21]. (To simplify the presentation of the regions, the explicit temperatures $(T_m^\circ)_{meta}$ and T^+ (the cross-over T) are taken as defining the boundary between regions. In reality region (i) will start somewhere below $(T_m^\circ)_{meta}$, and region (iii) will start somewhere below T^+).

[4] Salient topical examples include monotropic liquid crystals in polymers where the *monotropicity* itself (i.e. appearance of the liquid-crystal state on cooling the isotropic melt but not on subsequent heating of the crystalline state arising therefrom) is a direct manifestation of what has just been stated. In fact, in a specific work on monotropic liquid-crystal polymers in this laboratory we actually determined rate curves such as those in Fig. 13 including the cross-over, and registered the three regimes (i), (ii) and (iii) morphologically [21]. The same is apparent from a recent account of the crystallization of polypropylene in two of its crystal forms, α and β, with the two growth rates crossing over [22]. In both of the above cases intriguing morphological effects appear in the vicinity of T^+, reflecting competition between the relevant two phases in each type of material.

and an upper bound. The T-region of dominance of the "meta" phase would here be rather restricted, apart from the fact that the conditions set on A are contrary to the normal expectation.

Taking $\beta_{meta} > \beta_{stable}$, cannot lead to the prevalence of the metastable phase (that is, Equation 9) at any temperature in the case of $\alpha_{meta} \leqslant \alpha_{stable}$, (Figs AII.5 and AII.6, Appendix II); it could, however, do so with a single cross-over point for $\alpha_{meta} > \alpha_{stable}$, which is a realistic possibility in terms of α (Fig. AII.4 in Appendix II). However, here the crossing over is at a very much lower temperature than for the previous single cross-over situation in Fig. 13 (see also Figs AII.1 and AII.2 in Appendix II), which means not only that the metastable phase would take over only at these much lower temperatures (in absolute terms), but it would also takeover at very substantial supercoolings in terms of the metastable phase itself. This is contrary to general experience (see also the cases quoted in Footnote 4); according to general experience, the metastable phase takes over quite closely below $(T_m^\circ)_{meta}$, which is consistent with Fig. 13 and (Figs AII.1, AII.2 in Appendix II). This is also reflected by our recent findings on PE at high pressures (dominance or exclusive appearance of the metastable hexagonal phase below the triple point). The above is in addition to the fact that Equation 11b would be violated, the validity of which is consistently borne out by the rest of the material on which this paper is based.

In summary, while none of the possibilities featured in Appendix II can be ruled out *a priori* (hence they deserve continuing attention), the possibility of satisfying both Equations 9 and 10, represented by Fig. 13 (and Figs AII.1, AII.2 in Appendix II), remains both physically the most realistic and in best accord with general experience. Consequently we shall keep this case as the basis of the discussions to follow.

7.3. Relation between rates and phase-stability diagrams

As already stated the connection between kinetics, i.e. rates, and thermodynamics (i.e. phase stability) is inherent through the role of the minimum stable size featuring in both fields. As regards the rates, the exponent in Equation 7 contains the barrier for nucleation, which in turn is related to the size of the critical nucleus, l^*, as expressed by Equation 6. It follows, therefore, that the phase which grows fastest is the phase with the smallest critical nucleus, l^*, and vice versa. On the other hand, as shown in Section 7.1, l^* defines the phase lines in the phase-stability diagram, by which thermodynamic stability and rate criteria become linked. In particular, it follows that for the intersections in Figs 12 and 13 $T^* \equiv T_Q$ (selecting the simplest case in making this point) hence $T^* \equiv T_Q$ and T^+, are directly related.

The rate curves in Fig. 13, and in Figs AII.1 and AII.2 in Appendix II, do not contain any size factor, hence by implication, they refer to an infinite phase size. For a connection with phase-stability diagrams, clearly, size needs introducing. Doing this fully would require the introduction of a third axis, $1/l$, in Fig. 13, as in Fig. 8; this will not be followed through here. For the present purpose, it should suffice to say that assignments of rates as, for example, Fig. 13, can only apply from the critical size upwards, since below this size, l^*, the rate is zero. After taking note of the above it will be apparent that regions A_1, A_2 and B in Fig. 6 relate to regimes (i), (ii) and (iii) in Fig. 13 respectively, and vice versa, by T^+ being related to T_Q (they could be identical, or they could be related by a simple numerical factor or functionally[5]). Taking these regime relations in turn: the identification of A_1 with (i) is self-evident as the region where only the ultimately stable phase can exist. The same holds for the identification of region B with (iii); the latitude in its upper limit, as expressed in Footnote 5, has to be taken into account. The connection between region B and (iii) is possibly the most significant outcome of the present deliberations. The connection between A_2 and (ii), however, requires further consideration. Specifically, how far is there any phase development which is *truly* metastable (that is, without any size-determined stable region) which would be represented by, say, the M-phase in region A_2 in Fig. 6. This aspect was not considered in Section 4 where only growth in stable phases, including size-determined stability, was considered, and consequently compounded A_2 with A_1 as the collective region A, where phase transformation proceeds directly into the ultimately stable C-phase. Clearly, by rate considerations (Fig. 13), as opposed to pure-stability (Fig. 6) considerations the possibility of finite growth rates also in the metastable phase (M in Fig. 6) within region A_2 needs to be taken into account. In that case, for symmetry reasons, we also need to consider the possibility of metastable phase growth below T_Q, that is, finite growth rates of the size-determined metastable C-phase within the size-determined M-stability regime in region B. This actual phase competition by rates will be compounded with all the other factors, and it will not be pursued here further.

[5] For the precise relation between the kinetic and thermodynamic quantities referred to above the following need noting.

The relevant critical nucleus size for the kinetic considerations (Equation 6) is the one relating to the maximum of the free-energy barrier, that is where $\frac{\delta \Delta G}{\delta l} = 0$ which we denote as l_b^*, while that pertinent for the phase-stability diagram, (Figs 5 and 6) is the minimum size (for which we retain the notation l^*) for thermodynamic stability; that is, when $\Delta G = 0$. However, l_b^* and l^* are simply related: $l^* = 3/2 l_b^*$ for primary nucleation and $l^* = 2l_b^*$ for secondary nucleation. Thus, except for a multiplying factor, the argument linking kinetics and thermodynamics remains unaffected. A constant multiplier also relates T^* in Fig. 12, T^+ in Fig. 13 and T_Q in Figs 5 and 6, in the case of secondary nucleation. As arising from the higher power of σ in Equation 8, however, this multiplier becomes temperature dependent for primary nucleation owing to the higher power of ΔT in Equation 7.

While the above will need to be considered for numerical correlation of kinetic and thermodynamic data, it does not affect the conceptual content of the scheme.

7.4. A new look at Ostwald's rule of stages

Ostwald's rule of stages [20], now largely forgotten or by-passed as archaic, was frequently invoked in the earlier literature on phase transformations. It was usually quoted as stating that transformations between two stable phases occur through intervening stages of metastable phases, whenever such metastable phases exist.

Such explanations of the stage rule which exist have been on kinetic grounds (see below) "reducing" Ostwald's original conception of an intrinsic feature of matter to an issue of competing rates. We shall continue to maintain this here, while also linking it to size-dependent stability, thus also providing it with a thermodynamics-based foundation.

The first attempt to justify the stage rule is due to Stranski and Totomanov [23]; they invoked kinetic reasoning, namely, that metastable phases develop faster in the sequence of their "degree" of metastability, (metastability here refers to infinite phase size in the sense of conventional equilibrium thermodynamics). Specifically, they invoked the competition between rates of nucleation using expressions essentially equivalent to Equation 7. However, they neglected the differences between the ΔT- and T-dependences in the nucleation rates of the competing phases; hence they had no crossing of rates (such as in Fig. 13), and hence they had no upper bound to the validity of the stage rule. The latter was incorporated much later in the more comprehensive (and more correct) treatment of the same issue by Gutzow and Toschev [24]. This is, to our knowledge, the last word on the subject. The kinetic part of our own argument (Section 7.2.) is essentially equivalent to their treatment, hence it can similarly provide a kinetic underpinning of the stage rule, while also defining its limits of validity.

A connection between the stage rule and our phase-stability diagram has already been alluded to in Section 7.1. Provided that Equation 3 is satisfied, below T_Q (that is, in region B) the phase transformation must, by thermodynamic reasoning, start and proceed via an intermediate phase, such as would become metastable on achieving macroscopic size, whenever such phases of intermediate stability exist. In view of the correlation between region B in the phase-stability diagrams and the rate regime (iii), we can now restate the stage rule as stating that, in the transformation from one equilibrium phase stage to another, the phase which forms first is the phase which is stable down to the smallest size; in which case it will also develop fastest. If phases of intermediate ultimate stability exist (that is, such as are metastable when attaining infinite size) then *under specifiable conditions* it will be these phases which will form and develop in a sequence of their metastability by the above criterion. This links up with the rule of stages expressed in Ostwald's formulation.

The italics in the preceding sentence refer to the various limits within which the above contention is valid. Foremost is the adherence to Equation 3 which underlies everything. Or put another way, the fact that experimentally Ostwald's rule of stages is in evidence at all we may now, in the light of the present interpretation, take as support for the widespread validity of Equation 3 on which the above interpretation rests. To our knowledge there is no general law pertaining to the comparative magnitudes of the quantity $(\sigma/\Delta H)$ in terms of the stability of phases on an *a priori* basis. This would need to be argued for each specific case separately (as indeed will be done in this paper for PE – see Appendix III), yet on the basis of the widespread applicability of the stage rule, coupled with its justification as here presented, one may, with confidence, endow Equation 3 with wider generality than merely being an attribute of some specific feature of a specific material (as, for example, the fold surface of PE crystals).

Finally, Ostwald's rule of stages, in its original formulation, relies on the observability of the metastable phases in their macroscopic state. This means that it refers to infinite size, that is, to $1/l = 0$, which in Figs 5 and 6, is the T-axis alone. This in turn implies that there is no further change in phase in the course of growth, specifically in the M → C transformation in the notation of Figs 5 and 6. Should an M → C transformation occur, the whole growth history would be obliterated as far as is assessable from the final product. Short of monitoring the structure during growth, we would not even be aware of the existence of an intermediate M-phase, hence we would have no reason for invoking the stage rule. The same holds for the rates (Fig. 13); a "meta → stable" transformation during growth would cover up the influence the metastable state has had on the rate of the full phase transformation, unless the rates are monitored in the course of the overall transformation itself. At this point, one of the merits of the present scheme becomes apparent: amongst others, it incorporates the possibility of transient phases during transformation from one (ultimately) stable state to another under conditions which otherwise might remain unrecognized. In terms of the stage rule it widens the limits of the proviso "if such exists" (that is, metastable phases), and thus of the range of validity of the stage rule itself.

Polymers represent an interesting special case. Namely, here the two phases, C and M, lead to readily recognizable differences in the final morphology. Thus a transient M-phase should leave its mark in the final product even after an M → C transformation, which from experience always occurs, say in PE, in the form of arrested thickening growth of the lamellae. These lamellae, dependent on the stage where the primary growth had been arrested, may resemble extended-chain type or (intrinsically) chain-folded lamellae in terms of the traditionally applied criteria. In fact, it was the recognition of the latter possibility which set us on the present track.

However, between the two extremes (namely, full retention of the starting phase in its metastable form within the final sample, and its total disappearance due to complete transformation into the ultimately stable phase), there is the intermediate possibility of the simultaneous presence of both phases in the final product, or at least during the overall phase transformation. A few comments will be made on this point in what follows.

7.5. Competition between phases

When two or more phases are present in the final product, all but one will, necessarily, be in metastable states. As this situation is actually observed in solids (for example, whenever polymorphs are seen together, such as in say α- and β-polypropylene), it calls for attention.

In principle this situation could arise in two ways: (a) due to competition in rates, or (b) due to partial conversion during growth.

(*a*) *Rates.* As commented on further above, cross-over points such as in Fig. 13 are regions of potential competition between phases on a rate basis alone (that is, without invoking the size dependence of stability). Indeed, two examples have been quoted above in Footnote 4 relating to T^+ (upper cross-over temperature). If and when a second cross-over in rates also exists, (see Fig. AII.3, Appendix II) a similar situation is expected in the (much lower) temperature region around it.

(*b*) *Partial conversion.* When the growing phase is truly metastable (as, for, example M in the C-stability regime of region B in the phase-stability diagram in Fig. 5), it could transform at some stage during growth. The driving force will be the degree of metastability (that is, the supercooling, ΔT_{tr}, or in terms of Fig. 6 how far we are beyond l^*_{tr} along $\leftarrow$ B) in a transformation which otherwise is kinetically determined. In terms of the rate (Fig. 13), on transformation we change from a point along the curve "meta" (the point being defined by the prevailing growth temperature) to the corresponding point along the curve "stable" with the phase transformation continuing at the correspondingly slower rate of the stable phase. As the overall rate of the "meta → stable" transformation itself is finite, there will be two phases present simultaneously at any instant: their relative amounts will be determined by the ratio of the two individual growth rates (that is, that of "meta" and "stable") and by the rate of transformation between them (that is, "meta" → "stable"). With a finite transformation rate, eventually the whole material will be in its state of ultimate stability. Even so, particularly in the case of polymers, where the growth in the two alternative phases leads to distinctly different morphologies, it remains important to know what fraction of the material has been in one or the other of the two alternative phases before the liquid → solid transformation (that is, the primary crystallization, meaning the consumption of all liquid material) itself was complete, since this determines the overall morphology of the final product.

Note that (a) and (b) are basically different. In (a) the competition is directly by the primary transformation rates, while in (b) it is via the intermediary of the "meta → stable" transformation not relating to the primary rate in any direct manner. This point will be recalled in discussion of the specific case of PE in Section 9.

Finally, we make a comment on the continuing growth of the phase which has already transformed into its state of ultimate stability. Say phase C has arisen along the pathway of arrow B in Fig. 6 through transformation of the initially formed M-phase. If the growth is itself nucleation controlled, then the formation of the secondary nucleus will again be subject to the size-dependent alternatives of C and M, which are themselves subject to phase-stability considerations, such as in Fig. 6, but here applied to the growth surface of the pre-existing C-phase. By the preceding arguments, the new phase to arise, in this case along the surface of the C-phase, will be the phase which is stablest down to the smallest size, which, if we are below the appropriate T_Q, will be the M-phase. This would lead to the situation where the C-phase, originally arising through transformation from the M-phase, could continue to grow again through the M-phase. The latter, after attaining sufficient size, would then again transform into the C-phase, and so on. However, the stability conditions, hence the corresponding phase-stability diagram, will now need modification due to the presence of the C–M interface. This will raise the free energy, hence will reduce the stability of the M-phase arising under these circumstances. This results in depression of T_Q, and hence in widening region A. From Section 4, this will favour direct growth by C and conversely, disfavour growth by the intermediary phase, M. Nevertheless the latter will remain a possibility subject to the temperature and the other parameters involved; this calls for individual attention in each case.

8. Wedge-shaped crystals

It is a well-documented fact, in the subject of crystallization of PE under pressure that the lamellae have wedge-shaped cross-sections, at least up to the stage where they impinge face to face. This has always been interpreted as growth starting with chain folding at the leading edge, with gradual thickening up to full chain extension behind the growth front. Thanks to our improved electron micrographs and the use of sharp fractions and the strictly isothermal and isobaric conditions adopted [1–4, 25] we can now map actual wedge profiles to good accuracy and relate them both to the time of growth and to the now more precisely defined molecular lengths [3, 4, 25]. The former enabled us to identify actual thickening growth rates (note, this is now primary crystal growth in the thickness direction, not the generally considered thickening which is a rearrangement of the crystal already formed) and also to ascertain that such thickening growth proceeds beyond full chain extension, apparently indefinitely and without any discontinuity, until terminated by impingement on other growing crystals.

All the above takes place while in the h-phase irrespective of whether it is stable or metastable according to the phase regime. When metastable, there will be, at some stage, a h → o transformation, when according to the foregoing all growth, lateral and thickening, stops – as embodied by growth in region B of Fig. 6.

For simplicity, the sketch in Fig. 6 was constructed for parallel-sided platelets. Introduction of the wedge

shape leads to further issues of potential relevance beyond PE, hence its inclusion here.

The application of mode-B growth to a wedge would imply that the h → o transformation (in the specific case of PE) would commence at the thickest region of the continuously thickening wedge and then run down towards the thin extremity coming to a halt when the lowest thickness for which o is the stable phase (l^*_{tr} in Fig. 14) is reached. This would leave the thinnest extremity of the wedge untransformed, hence in the h-phase, which by all the foregoing could then continue to grow with its rate unaltered. This is contrary to observation, according to which, upon transformation, all growth, lateral and thickening should cease (or drastically slow down).

The way out of the problem is to consider the h–o interface within the transforming crystal. As such an interface represents additional free energy, the transformation will try to reduce it, which it can by the transformation front moving towards the thinner part of the wedge where the cross-sectional area, hence the total interfacial energy, is smaller. It will be apparent, even qualitatively, that the front will pass below the thickness, l^*_{tr}, that is, into the region where, for a parallel sided plate, the h-phase, and not the o-phase, will be stable. It will come to a halt at some $\bar{l}$ where the reduction in the h–o interfacial energy no longer compensates for the creation of more volume of the o-phase, (which in the absence of the h–o interface would have a higher free energy than the h-phase in the l-range in question). If this $\bar{l}$-value, at which the transformation becomes arrested, is below the stability limit of the h-phase ($l^*_h \equiv l^*_M$, in Fig. 14) all growth will stop, accounting for our observations.

The criterion was derived in [3]. This is

$$\bar{l}\Delta f \cos\theta > \Delta\sigma_e - 2\sigma_i \sin\theta \qquad (14)$$

where Δf is the change in bulk free energy and $\Delta\sigma_e$ is the change in the basal-surface free energy on transformation, σ_i is the interfacial surface free energy (that is that of the h–o surface for PE) and θ is half the wedge angle.

If, in addition to Equation 14, the right-hand side is also zero or negative, that is,

$$\Delta\sigma_e \leqslant 2\sigma_i \sin\theta \qquad (15)$$

then Equation 14 will hold for all l; hence the transformation will run down to the wedge tip, irrespective of the thickness of the tip.

The implications of the above are discussed in [3]; here we shall place them within the framework of our (T, $1/l$)-phase-stability diagram, as represented by Fig. 6, as an instructive application of the foregoing.

Fig. 14 represents a wedge section parallel to the taper direction. Marked are the thickness positions (l values) l^*_{tr}, l^*_o and l^*_h corresponding to l^*_{tr}, l^*_{Cb} and l^*_M in Fig. 6. The h → o transformation will start somewhere corresponding to $l^+ > l^*_{tr}$. If, $\bar{l}$ as defined by Equation 14, is smaller than l^*_h then the transformation will run to the outer extremity engulfing the full wedge, thus leaving no h–o interface. As l^*_h is the stability limit of the h-phase its further growth, and with it that of the whole wedge-shaped crystal, becomes arrested. It should be further noted that between l^*_{tr} and l^*_o the o-phase is unstable with respect to the h-phase (as referred to parallel-sided plates) but it is still stable with respect to the L-phase (melt); that is, the o-phase is metastable. For still thinner portions, that is, for $l < l^*_o$, o also becomes unstable with respect to the L-phase and it cannot persist any longer. Hence, we should have the rather unusual situation that the h → o transformation should first run to the wedge end, eliminating all the h-phase, and then the wedge extremity (now all in the o-phase) will melt back to the thickness corresponding to l^*_o where the o-phase becomes stable with respect to the melt. Note that here it will still remain unstable with respect to the h-phase, but the latter cannot form because of the requirement for creating an h–o interface. Formation of a high-energy surface is of course the requirement in all nucleation; however, in the present case of a wedge geometry, the (interfacial surface)/(volume) ratio will remain constant on an increase of the volume of the new phase (that is, on spreading of the h-phase upwards along the wedge), hence the nucleation barrier due to the surface cannot be overcome by growth of the new phase.

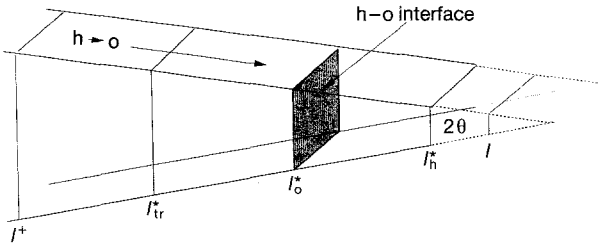

Figure 14 Phase transformation in a wedge geometry, drawn for a thickness-dependent h → o transformation pertaining to PE. l^+ is the kinetically determined transformation thickness within the o-stability regime l^*_o, l^*_h, l^*_{tr} represent the respective critical stable lengths for the formation of the o- and h-phases (from the melt) and for the o → h solid–solid transformation, pertinent for parallel-sided entities. The o–h interface is indicated chosen here to lie at l^*_o. The transformation (here h → o) can proceed down to thicknesses which are smaller than defined by thermodynamic stability criteria for parallel faces, and could even run to the wedge tip, due to the gain in stability arising from reduction of the solid–solid (here h → o) interface, which in a wedge geometry remains partially uncompensated by the formation of greater volume (see the text).

Clearly the above conditions of phase transformation within a wedge geometry are most intriguing. They can explain our observations close to the triple point, namely that both thickening and lateral growth steps (or slows down) on h → 0 transformation [1, 2], while through Equation 14 it still allows for the possibility of continuing lateral growth after cessation of thickening growth following the h → 0 transformation under appropriate crystallization conditions when, for example, lateral growth is seen to proceed uninterrupted (as at atmospheric P–see Section 9). The above principles on wedge shapes should be of wider generality. *Mutato mutandis*, they should hold for all materials, and not only for crystallization but also for other phase transformations, liquid–liquid and gas–liquid (and capillary condensation?). The above considerations are expected to have consequences for material

behaviour within pores and cracks, wherever tapered confines prevail, an issue of potential practical consequence.

9. Applicability of the scheme to the crystallization of PE

The question clearly arises as to how far existing experiences with the much studied PE – the system serving as a basis for understanding the crystallization of flexible polymers – are affected by the foregoing considerations. Specifically, does, or can, crystallization at atmospheric pressure conform to mode-B crystallization as opposed, or in addition to, mode A, which has always been implicitly taken for granted? This issue will be scrutinized in what follows. We state to begin with, that mode-B crystallization will emerge as a strong possibility for crystallization from the melt, while mode A remains a plausible mode for crystallization from solution (as always implicitly assumed). For answering the question posed, we need to construct the T versus $1/l$ phase-stability diagram at $P \sim 0$. Specifically, we need to assess first as to whether it is of the type as in Fig. 5 (that is whether the o- and h-lines intersect); the condition for this is that Equation 5 holds. If so, the point of intersection, T_Q needs to be located as it is the most relevant parameter.

For the above, we need to know the relevant input parameters, $(T_m^\circ)_o$, $(\Delta H)_o$, $(\sigma_e)_o$, $(T_m^\circ)_h$, $(\Delta H)_h$, $(\sigma_e)_h$, T_{tr}^0, $(\Delta H)_{tr}$ and $(\sigma_e)_{tr}$. Of these $(T_m^\circ)_o$, $(\Delta H)_o$ and $(\sigma_e)_o$, are known to a reasonable precision as a result of extensive past works on crystallization and melting in the o-phase along traditional lines. They are the results of measurements coupled with extrapolation to $l = \infty$ $[(T_m^\circ)_o, (\Delta H)_o]$ and of fitting procedures with theories $[(\sigma_e)_o]$. This is common knowledge, and needs no further comment. Values of (ΔH) and (T_m°) for the other transitions can be assessed from data available from the literature facilitated by the fact that the values for the three states are not independent, so that only two of the three states need to be known separately.

We can find well-founded estimates in the literature for T_{tr}^0 and $(\Delta H)_{tr}$. Even if T_{tr}^0 is virtual at atmospheric pressure, o → h transformation has been observed in cases where the system could be superheated. Such situations can arise in highly oriented fibres which are constrained so that relaxation to a fully disordered melt is prevented. The constraints may only need to be external (clamping, embedding, see, for example [26]) but they can also be enhanced by internal cross-links introduced by radiation (see, for example, [27, 28]). The o → h transformation was found to occur in the range 145–151 °C, mostly at the upper end of the range. Accordingly we may take 150 °C as a reasonable value for T_{tr}^0 at atmospheric pressure.

In works on melting of radiation cross-linked fibres, Hikmet *et al.* [27, 28], in addition to observing the o → h transition as such, also determined the heats of fusion of the phases involved. Accordingly, $(\Delta H)_h = 160\ \text{ergs cm}^{-3}$, hence $(\Delta H)_h = 0.57(\Delta H)_o$. We recognize that such a value for $(\Delta H)_h$ may appear rather high, but since the precise value of $(\Delta H)_h$ will not affect our overall arguments we prefer to use this experimentally based value. Now, using the further relations that $(T_m)_\alpha = (\Delta H)_\alpha / \Delta S_\alpha$ (here α stands for any chosen structure) and $\Delta H_o = \Delta H_h + \Delta H_{tr}$ and $\Delta S_o = \Delta S_h + \Delta S_{tr}$, we can obtain a reasonable estimate for the equilibrium melting points $[(T_m^\circ)_h = 138\,^\circ\text{C}$, $T_{tr}^\circ = 150\,^\circ\text{C}]$ as well as the heats of fusion $(\Delta H)_\alpha$ of both phases and also the heat of transition, $(\Delta H)_{tr}$. Other reported values in the literature are all closely in the same range [27].

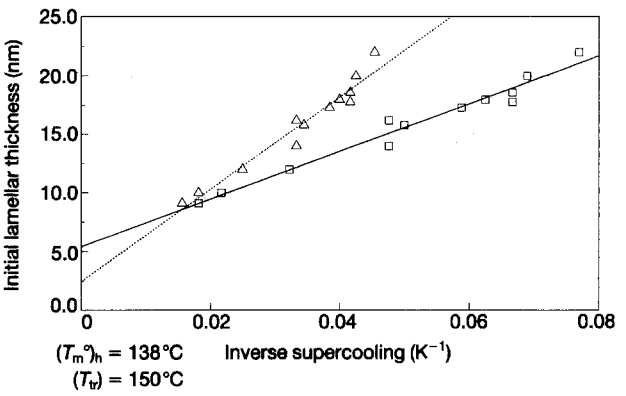

Figure 15 The variation of the initial lamellar thickness of melt-crystallized PE plotted according to (—□—) Equation 16 (where the supercooling is from the h-phase melting (temperature), and (--- △ ---) Equation 17 (where the supercooling is measured from the h → o transformation.

The remaining open-ended problem is that of σ_e. With $(\sigma_e)_{tr} = (\sigma_e)_o - (\sigma_e)_h$, $(\sigma_e)_h$ is left as the only unknown quantity – on which everything else will hinge. Here we can take three routes. (1) Assume that mode-B crystallization applies to cases where l_g^* is known, and test for self-consistency with experimental T_c versus l data when applying the theoretical relationship between T_c and l^*. In addition to telling us whether the assumption of mode-B crystallization is valid or not, this will provide a value for $(\sigma_e)_h$ when it is valid. (2) We may test for the validity of a phase diagram such as Fig. 5 and for the feasibility of having mode-B crystallization at $P \sim 0$ by choosing specific input values, such as would yield this mode of crystallization, and assess whether such values are feasible from other considerations. (3) We may try to estimate $(\sigma_e)_h$ from *a-priori* considerations in the light of present knowledge. We shall pursue routes 1 and 2 in what follows. The results of route 3, as will be seen, slots into the discussion on route 2 but its derivation will be deferred to Appendix III.

9.1. A test involving self-consistency

Take the available minimum value for l at a given T_c, and, assuming that crystallization has been within mode-B, we shall consider two possibilities. (i) The l-value in question corresponds to $(l^*)_h$, when, by existing theories,

$$(l^*)_h = \frac{2(\sigma_e)_h T_m^\circ}{(\Delta H)_h (\Delta T)_n} + \delta l \qquad (16)$$

(ii) This corresponds to $(l^*)_{tr}$ when

$$(l^*)_{tr} = \frac{2(\sigma_e)_{tr} T^\circ_m}{(\Delta H)_{tr}(\Delta T)_{tr}} \quad (17)$$

with $(\sigma_e)_{tr} = (\sigma_e)_o - (\sigma_e)_h$

Our source of data will be from latest works on crystallization from the melt [29] aimed at assessing l by low-angle X-ray scattering at as early a stage of crystallization as possible so as to forestall, or to minimize, the effect of thickening, and thus to assess the initial thickness of the crystal, that is, $(l^*_g)_h$ (high-power-synchrotron-generated X-rays were used on samples of maximized nucleation rates to obtain a diffraction signal in minimum time). In that study, a minimum value for l was found which rapidly increased by doubling or tripling in thickness. We may now assume that the minimum thickness was either l^*_h, the absolute minimum possible, that is, (i) above, to which Equation 16 applies. Alternatively, we may assume that at the stage of observation the crystals have already transformed to the o-phase where primary thickening growth has already been arrested, and the further secondary thickening occurs much more slowly and, in this case, in integer steps. The smallest l at which this could occur is l^*_{tr}; this corresponds to case (ii) and the corresponding relation of Equation 17.

To obtain $(\sigma_e)_h$, the experimentally determined minimum l-values were plotted against $(\Delta T)^{-1}$ for both cases (i) and (ii) using Equations 16 and 17, respectively (with ΔT being different for the same T_c-value in the two cases). As seen from Fig. 15 there is a reasonable fit to straight lines, showing that the functional relations in Equations 16 and 17 are obeyed. This remains true whether we choose the high $(T^\circ_m)_h$-value of 138 °C or a lower $(T^\circ_m)_h$ of say 131 °C. The $(\sigma_e)_h$-values themselves can then be obtained from the gradients of the lines. They are $(\sigma_e)_h = 40.5\ \text{erg cm}^{-2}$ and $(\sigma_e)_h = 37.0\ \text{erg cm}^{-2}$ for cases (i) and (ii), respectively. These values yield the respective values of 0.763 and 0.69 for the ratio $(\sigma_e/\Delta H)_h/(\sigma_e/\Delta H)_o$. This satisfies Equation 5, and the existence of a B-mode follows. It is noteworthy that the ratio is smaller (hence the inequality is more pronounced) for case (ii), which in turn means that the region of mode B extends to higher temperatures and hence it will be more prominent and more readily accessible. It follows, therefore, that case (i) is the most stringent limit for the existence of mode B. Thus, by confining ourselves to case (i), we represent the least favourable case for region B. Case (ii), or any other choice, say $o \rightarrow h$ transformation at $l > l^*_{tr}$, will enhance the role of mode B still further.

We should note here that a different picture emerges when we consider crystallization for solution. If we use the same values for $(\sigma_e)_o$, $(\Delta H)_o$, $(\Delta H)_h$ and T^0_{tr} as for melt crystallization but reduce $(T^\circ_m)_o$ from 145 °C to 112 °C and then recalculate T_Q, we find that T_Q drops to around 20 °C; that is, it is outside the usual range of crystallization temperatures. Thus we should expect mode-A crystallization to dominate the behaviour of PE crystallized from solution.

9.2. A test involving systematic variation of input parameters

Here we wish to show the wide range of possible values for $(\sigma_e)_h$, $(\Delta H)_h$ and $(T^\circ_m)_h$ which do in fact lead to crystallization of PE in mode B. To find the triple-point temperature, T_Q, by applying Equation 4 we need values for $(T^\circ_m)_h$ and the ratio, $X = [(\sigma_e)_h/(\Delta H)_h]/[(\sigma_e)_o/(\Delta H)_o]$, which, of course, from Equation 5, must be less than unity. We show in

TABLE I Triple point temperatures for polyethylene

$\frac{(\sigma_e)_h}{(\Delta H)_h} / \frac{(\sigma_e)_o}{(\Delta H)_o}$	0.15	0.24	0.34	0.43	0.53	0.62	0.72	0.81	0.90	0.99	
$(\sigma_e)_h/(\Delta H)_h$	5×10^{-8}	8.1×10^{-8}	1.1×10^{-8}	1.4×10^{-8}	1.8×10^{-8}	2.1×10^{-8}	2.4×10^{-8}	2.7×10^{-8}	3×10^{-8}	3.3×10^{-8}	cm^{-1}
$(\sigma_e)_h$	8	13	18	23	28	33	38	43	48	53	erg. cm^2
$(T^\circ_m)_h$ °C											
125	*121.7*	*119.0*	115.5	111.0	104.9	96.1	82.3	57.9	2.1	− 251.7	
126	*122.8*	*120.2*	*116.9*	112.6	106.8	98.3	85.1	61.5	7.1	− 250.7	
127	*124.0*	*121.0*	*118.4*	114.3	108.7	100.6	88.0	65.2	12.3	− 249.4	
128	**125.1**	*122.8*	*119.8*	*116.0*	110.6	103.0	90.9	69.0	17.7	− 248.1	
129	**126.3**	**124.1**	*121.3*	*117.6*	112.6	105.3	93.8	72.9	23.2	− 246.6	
130	**127.5**	**125.4**	*122.7*	*119.3*	114.5	107.6	96.7	76.8	28.9	− 244.8	
131	**128.6**	**126.7**	*124.2*	*120.9*	*116.5*	110.0	99.7	80.8	34.8	− 242.9	
132	**129.8**	**128.0**	**125.6**	*122.6*	*118.4*	112.4	102.7	84.8	40.9	− 240.7	
133	**130.9**	**129.3**	**127.1**	*124.3*	*120.4*	114.8	105.7	88.9	47.2	− 238.2	
134	**132.1**	**130.6**	**128.6**	**126.0**	*122.4*	*117.2*	108.8	93.2	53.7	− 235.2	
135	**133.3**	**131.9**	**130.1**	**127.7**	*124.4*	*119.6*	*111.9*	97.4	60.5	− 231.7	
136	**134.4**	**133.2**	**131.5**	**129.4**	**126.4**	*122.1*	*115.0*	101.8	67.6	− 227.5	
137	**135.6**	**134.5**	**133.0**	**131.1**	**128.4**	*124.5*	*118.2*	106.2	74.9	− 222.4	
138	**136.8**	**135.8**	**134.5**	**132.8**	**130.5**	**127.0**	*121.4*	110.8	82.9	− 216.0	
139	**138.0**	**137.1**	**136.0**	**134.5**	**132.5**	**129.5**	*124.7*	*115.4*	90.3	− 207.9	
140	**139.1**	**138.4**	**137.5**	**136.3**	**134.6**	**132.1**	**128.0**	*120.1*	98.5	− 197.1	
141	**140.3**	**139.7**	**139.0**	**138.0**	**136.6**	**134.6**	**131.3**	*124.9*	107.1	− 182.0	
142	**141.5**	**141.0**	**140.5**	**139.7**	**138.7**	**137.2**	**134.7**	**129.7**	*115.9*	− 159.7	
143	**142.6**	**142.4**	**142.0**	**141.5**	**140.8**	**139.8**	**138.1**	**134.7**	**125.2**	− 123.1	

Table I calculations of the triple-point temperature, T_Q, for a range of $(T_m^\circ)_h$ from 125 to 143 °C and of the ratio X from 0.15 to 0.99. We may calculate from X, the ratio $(\sigma_e)_h/(\Delta H)_h$, and if we choose the literature values for $(\Delta H)_h$ referred to in the previous section we may also calculate $(\sigma_e)_h$; these calculated values are also shown in Table I. We should note that if we choose a low value of $(\sigma_e)_h$ of around 8 erg cm^{-2} (as proposed by the considerations presented in Appendix III) then T_Q will fall in the usual range of crystallization temperatures for PE provided that $(T_m^\circ)_h$ is greater than 130 °C. We have delineated three regions within Table I. The data in bold type indicate $T_Q > 125$ °C, that is, where T_Q falls within the normal range of crystallization conditions for PE. We should expect mode-B crystallization to occur commonly at atmospheric pressure in PE if the corresponding values for $(T_m^\circ)_h$ and $(\sigma_e)_h/(\Delta H)_h$ are correct. The data in italic type indicate $115 < T_Q < 125$ °C; in this case we would expect occasional mode-B crystallization and/or competition between the A- and B-modes. Finally the data in normal type, indicating $T_Q < 115$ °C, show the range of $(T_m^\circ)_h$- and $(\sigma_e)_h/(\Delta H)_h$-values for which we would not expect mode-B crystallization at all.

In summary, we see from Table I that there is a wide latitude of input parameters which would permit the crystallization of PE melts to take place by mode B at atmospheric pressure, suggesting that such a possibility needs at least to be considered.

It should be remarked that preference for mode B, that is, for primary formation of h-crystals, need not exclude the coexistence of h- and o-crystals even during the crystallization process itself. This situation has actually been reported for high-pressure experiments as T_c is lowered [7]. This would arise from kinetic considerations through competition by rates (see Section 7.5). However, if the physically most plausible rate situation pertains, such as is represented by Fig. 13, this will not be through competition of primary rates (case (a) in Section 7.5) as lowering of T_c will increasingly favour the h-phase, but through the increasing rate of the h → o conversion as embodied by case (b) in Section 7.5. It follows that in such a situation the L → h crystallization will not be increasingly replaced by the L → o crystallization on lowering T_c, as might be implied [7]; on the contrary, it will be enhanced, only its life span will be reduced with all the consequences for the morphology of the final product.

To sum up, Section 9: while there is no certainty at this stage, the possibility emerges that the crystallization of PE from the melt, at atmospheric pressure, could well occur via mode B instead of by mode A as has always been assumed in the past. The implications of this conclusion are potentially far reaching, inviting further considerations. The least we can say with certainty is that the possibility of a B-mode crystallization from the melt is internally self-consistent and does not lead to any obvious contradictions. However, previous considerations on crystallization from solution, the starting point of the whole subject area of chain-folded crystallization, and that of the first theories set out to account for it [30], would remain unaffected by the new considerations presented here.

10. Conclusion

As has been shown, invoking the size dependence of phase stability has profound potential implications for phase transitions in general and for crystallization in particular, with polymers, the subject of our own interest, representing a particularly special situation. Namely, when different polymorphs can exist then the size dependence of their stability with respect to the melt and to each other will, in general, be different. This can, under certain specified, but apparently frequently realized, conditions, lead to inversion of stability with the phase dimension. Thus, for sufficiently small sizes, a phase which would be metastable for infinite size – as usually represented in equilibrium phase diagrams – could become the stable phase. This situation is clearly of major consequence for the process of phase transition, and crystal growth in particular, because it means that the new phase passes through different regimes of thermodynamic stability in the course of growth. In particular, it would start life in a phase, which at that stage of growth is of maximum thermodynamic stability, but would become metastable as the phase reaches macroscopic dimensions. It may remain in this, by this stage metastable phase, when it would appear to obey Ostwald's rule of stages; or it may transform to the phase of ultimate stability, consequently covering up the history of its growth (thus, amongst others, making theories or models of growth relying on this final stage alone insufficient).

The above, purely thermodynamic, consideration can be readily linked up with the kinetics of growth in the case that the latter is nucleation (primary or secondary) controlled. Namely, here the fastest growth path will be the one which proceeds through the smallest stable critical nucleus (primary or secondary), which in turn corresponds to the phase having the lowest free energy for the smallest dimension at that particular supercooling. These considerations provide a ready explanation for Ostwald's rule of stages, now based on combined kinetic and thermodynamic considerations, while also defining the supercooling range where the stage rule is expected to be obeyed. In the latter context, the kinetic competition between stable and metastable phases can (see Appendix II) now be assessed from a comprehensive viewpoint.

The above leads to specific consequences in the field of chain-folded crystallization of polymers; or, conversely, several so far largely disconnected experimental findings in polymer crystallization can now be brought under a unifying conceptual umbrella on the basis of the above considerations. In polymers, the smallest, hence stability-determining, dimension is the lamellar thickness, l. Further, out of the possible crystal polymorphs there is usually a phase of high-chain mobility, most frequently diagnosed as a h-phase, intermediate between the ultimately stable crystal and the melt, which acquires special significance (as first pointed out by Bassett and recently reemphasized in

our own laboratories) in the course of crystallizing PE under pressure. In this mobile phase, the crystals grow in the thickness direction (thickening growth), thus increasing l through the mechanism of chain folding, progressively leading to full chain extension (through sliding diffusion) and to thicknesses beyond. Now, in the P and T range, where otherwise this mobile phase would be metastable (for infinite size), the situation described in the previous paragraph could arise; namely (parameters permitting) crystallization would begin in the mobile intermediate phase where it could then start from the smallest critical stable nucleus of size l(which here is the fold length) and proceed to grow both laterally, and being in the mobile phase also in the thickness direction. At a sufficiently large l (thickness) the crystal would pass into a different phase regime, into the regime of ultimate stability with lowered chain mobility. On transformation into this phase, at some stage along the growth path, thickening growth would stop or slow down drastically, thus locking in the crystal thickness at the stage where this transformation occurs. In that case, the lamellar thickness, as registered in the final product, would thus reflect a memory of the different initial phase in which the crystal originated, a feature which would be unique to chain-folded crystallization of polymers amongst all the other phase transformations and substances, to which the previous considerations would otherwise apply.

The assertion that phase transformation between two polymorphs can be induced by change in size has been verified, to our knowledge for the first time, in the case of a polymer, 1–4 *trans*-butadiene in support of the present basic considerations in general, and of the role of crystal thickening in a mobile phase for polymers in particular. For the case of the much studied PE, the usually observed chain-folded lamellar crystallization, and the rather specialized case of extended-chain-type crystallization under high pressure, can be combined in a unified picture through a (P, T, $1/l$)-phase-stability diagram defining the stability regime of the mobile h-phase where chain extension can occur in (P, T, $1/l$)-space (Fig. 8). Here, wherever the mobile phase is stable for $l = \infty$, the well-established situation for extended-chain-type crystallization remains valid. However, in the phase-space region where the stability of the mobile phase is size-limited (that is, l-limited), which includes the case of atmospheric pressure, the question arises as to whether crystallization proceeds, directly through the ultimately (that is, for $l = \infty$) stable orthorhombic phase (case A) or through the mobile h-phase as an intermediate transient (case B) (see Fig. 6). Case A is the situation always envisaged in the past, on which all models are based, while the case B brings in the totally new considerations outlined above. By a variety of arguments and through computations using input parameters based on plausibility and on consistency with experimental data, we conclude, at the present stage, that there is a strong possibility for case B pertaining for crystallization under atmospheric pressure in the case of the melt, while case A remains valid (as has always been considered) for crystallization from solutions. But we do not wish to be categoric on these issues; the essential point is that, for the first time, a new broadened scheme of possibilities has been recognized and presented and opened up for general scrutiny. Specifically, which mode of crystallization applies under which circumstance (that is, for P and T, and for melts and solutions)?

Further, attention was given to the role of the interface between the two crystal phases in the crystal → crystal transformations in the special, but experimentally observed, wedge-shaped crystals. It could be shown that in this special geometry (where the increasing volume of the newly formed phase may not compensate for the effect of the decreasing surface in the course of the transformation) the transformation may proceed down to sizes (that is towards the tip of the wedge) where otherwise, for parallel-sided systems, the newly formed phase would be unstable. This recognition not only strengthens the case for mode-B crystallization in PE in the light of the available evidence, but it is of potentially wider significance for phase transformations in confined tapering spaces.

Finally, an analytical treatment of the size, ($1/l$), dependence of triple points has led to the recognition of a singularity as a general feature of (P, T, $1/l$)-phase-stability diagrams, with consequences which have yet to be assessed (Appendix I).

Acknowledgement

A. Keller and G. Goldbeck-Wood gratefully acknowledge discussions with Professor R. Evans on the theoretical background.

References

1. S. RASTOGI, M. HIKOSAKA, H. KAWABATA and A. KELLER, *Macromolecules* **24** (1991) 6384.
2. M. HIKOSAKA, S. RASTOGI, A. KELLER and H. KAWABATA, *J. Macromol. Sci. Phys. B.* **31** (1992) 87.
3. S. RASTOGI, M. HIKOSAKA, A. KELLER, H. KAWABATA and A. TODA, in preparation (see also [30]).
4. S. RASTOGI, M. HIKOSAKA, H. KAWABATA and A. KELLER, *Macromol. Chem. Macromol. Symp.* **48/49** (1991) 103.
5. A. KELLER, in "Crystallization of polymers", edited by M. Dosière, Nato ASI-C series **405** (Klumer Acad., Dodrecht, 1993) p. 1.
6. D. C. BASSETT and B. TURNER, *Phil. Mag.* **29** (1974) 285.
7. *Idem., ibid.* (1974) 925.
8. M. HIKOSAKA, *Polymer* **28** (1987) 1257.
9. *Idem., ibid.* **31** (1990) 458.
10. A. KELLER and G. UNGAR, *J. Appl. Polymer Sci* **42** (1991) 1683.
11. V. PERCEC and A. KELLER, *Macromolecules* **23** (1990) 4347.
12. A. KELLER, G. UNGAR and V. PERCEC, in "Liquid crystalline polymers" edited by R. H. Weiss and C. K. Ober, ACS Symposium Series, Vol. **435** (Amer. Chem. Soc., Washington, 1990) p. 308.
13. K. ASAI, *Polymer* **23** (1982) 391.
14. J. D. HOFFMAN and I. J. WEEKS, *J. Chem. Phys.* **42** (1965) 4301.
15. B. WUNDERLICH and L. MELILLO, *Makromol. Chem.* **118** (1968) 250.
16. D. C. BASSETT, in "Developments in crystalline polymers", Vol. 1, edited by D. C. Bassett, (Applied Science, London, 1982), p. 115.

17. M. HIKOSAKA, K. TSUKIJIMA, S. RASTOGI and A. KELLER, *Polymer* **33** (1992) 2582.
18. S. RASTOGI and G. UNGAR, *Macromolecules* **25** (1992) 1445.
19. J. FINTER and G. WEGNER, *Makromol. Chem.* **182** (1981) 1859.
20. W. OSTWALD, *Z. Physik. Chem.* **22** (1897) 286.
21. D. HEBERER, A. KELLER and V. PERCEC, to be published.
22. J. VARGA, *J. Mater. Sci.* **27** (1992) 2557.
23. I. STRANSKI and D. TOTOMANOV, *Z. Physik. Chem. A* **163** (1933) 399.
24. I. GUTZOW and S. TOSCHEV, *Kristall und Technik* **3** (1968) 485.
25. M. HIKOSAKA, K. AMANO, S. RASTOGI and A. KELLER, in "Crystallization of polymers" edited by M. Dosière, Nato ASI-C series. **405** (Klumer Acad., Dodrecht, 1993) p. 331.
26. A. J. PENNINGS and A. ZWIJNENBURG, *J. Polymer Sci. Polym. Phys. Ed.* **17** (1979) 1011.
27. R. A. HIKMET PhD thesis, Bristol University, Bristol, UK (1985).
28. R. A. HIKMET, A. KELLER and P. J. LEMSTRA, to be published.
29. P. J. BARHAM and A. KELLER, *J. Polymer Sci. Physics Ed.* **27**, (1989) 1029.
30. J. D. HOFFMAN and J. I. LAURITZEN, *J. Natn. Bur. Stand. A* **64** (1960) 73.

Received 26 July
and accepted 26 August 1993

Appendix I: The dependence of the triple point on lamellar thickness

The point in phase space at which a pure substance exists simultaneously in three phases is called the triple point. If the interfaces between the respective phases are planar, the system is *invariant*, i.e. there are no extra degrees of freedom, and it can only exist in equilibrium at one point. If, however, the interfaces are curved, e.g. due to small size, the *variance* is equal to two [1]. This means that the triple point is a function of two variables whose values can be given arbitrarily.

The system the present paper is concerned with is that of a polymer liquid phase (L), a mesophase (M) and a crystal (C). The schematic phase diagram of this system is shown in Fig. 7. As already discussed, the two variables on which the triple point depends are the thicknesses of the crystal and of the mesophase lamellae. The aim of the following analysis is to provide a quantitative description of the link between the crystallization under high pressure and ambient conditions shown schematically in Fig. 8.

The following analysis is based on an analogy with the size dependence of the triple point of water (with ice and vapour) which was studied in detail by Defay *et al.* [1].

At equilibrium, the following conditions apply to the temperature, T, and the chemical potential, μ (per mole), of the different phases:

$$T_L = T_M = T_C \equiv T \quad \text{(AI.1)}$$

$$\mu_L = \mu_M = \mu_C \equiv \mu \quad \text{(AI.2)}$$

The hydrostatic pressure, P, is related to the end surface free energy, σ, and the lamellar thickness, l, of the respective phases by Laplace's law, assuming it is valid down to lengths of the order of 10.0 nm. As in the main text, it is assumed that the contributions of the lateral surfaces of the lamellar crystals can be neglected. Hence

$$P_M - P_L = 2\sigma_M/l_M \quad \text{(AI.3)}$$

$$P_S - P_L = 2\sigma_C/l_C \quad \text{(AI.4)}$$

The relation between the temperature, pressure and chemical-potential variations is given by the Gibbs–Duhem equations

$$-s_L\delta T + v_L\delta P_L = \delta\mu \quad \text{(AI.5)}$$

$$-s_M\delta T + v_M\delta P_M = \delta\mu \quad \text{(AI.6)}$$

$$-s_C\delta T + v_C\delta P_C = \delta\mu \quad \text{(AI.7)}$$

where s and v denote the entropy and the volume per mole, respectively.

The above set of equations (Equations AI.3–AI.7) contains six variables: three pressures, two thicknesses and the temperature. Four variables can be eliminated from these equations. If, in addition, the lamellar thicknesses of the stable and metastable phase are set equal to the same value, $l_C = l_M \equiv l$, equations for the variation of the triple-point temperature and pressure with the lamellar thickness can be derived.

First, the temperature variation, δT, of the triple point as a function of size shall be calculated. Therefore, the pressures and the chemical potential are eliminated. This yields

$$\left[\frac{\Delta s_C}{\Delta v_C} - \frac{\Delta s_M}{\Delta v_M}\right]\delta T = \frac{v_M}{\Delta v_M}\delta\left(\frac{2\sigma_M}{l}\right) - \frac{v_C}{\Delta v_C}\delta\left(\frac{2\sigma_C}{l}\right) \quad \text{(AI.8)}$$

Here and in the following, the difference of a quantity between the liquid state and either the stable or the metastable phase is denoted by Δ. The triple-point temperature of a curved system can now be obtained, in principle, by integration from the planar case, where $T = T_0$, and $1/l = 0$ to the lamellar case, where $T = T(l)$. It must be noted that the entropies, s, specific volumes, v, and surface free energies, σ, are all in principle temperature dependent. Since these dependencies are not known in detail, the following first approximations are applied: (i) the surface free energies and the specific volumes are set to constant values, and (ii) the differences in entropy are approximated by

$$\Delta s = \Delta h/T \quad \text{(AI.9)}$$

with a constant enthalpy, Δh, per mole. This will be replaced by the enthalpy per volume $\Delta H = v\Delta h$. The differential triple-point equation then takes the following form:

$$\left[\frac{v_C\Delta H_C}{\Delta v_C} - \frac{v_M\Delta H_M}{\Delta v_M}\right]\frac{\delta T}{T} = \left[\frac{2\sigma_M v_M}{\Delta v_M} - \frac{2\sigma_C v_C}{\Delta v_C}\right]\delta\left(\frac{1}{l}\right) \quad \text{(AI.10)}$$

This equation can be rewritten as

$$\frac{\delta T}{T} = -\frac{2\sigma_C}{\Delta H_C}\left\{\frac{[(\sigma_M v_M/\Delta v_M)/(\sigma_C v_C/\Delta v_C)]-1}{[(v_M\Delta H_M/\Delta v_M)/(v_C\Delta H_C/\Delta v_C)]-1}\right\}\delta\left(\frac{1}{l}\right) \quad \text{(AI.11)}$$

and on integration an exponential dependency of the triple-point temperature on size is obtained

$$T(l) = T_0 \exp(-l_T/l) \qquad \text{(AI.12)}$$

where

$$l_T = \frac{2\sigma_C}{\Delta H_C}\left\{\frac{1-[(\sigma_M v_M/\Delta v_M)/(\sigma_C v_C/\Delta v_C)]}{1-[(v_M \Delta H_M/\Delta v_M)/(v_C \Delta H_C/\Delta v_C)]}\right\} \qquad \text{(AI.13)}$$

In a similar way, the change in triple-point pressure with curvature can be calculated by eliminating $\delta\mu$, δT, δP_C and δP_M from Equations AI.3–AI.7. This yields

$$\left[\frac{\Delta v_C}{\Delta s_C} - \frac{\Delta v_M}{\Delta s_M}\right]\delta p = \left[-\frac{2\sigma_M v_M}{\Delta s_M} + \frac{2\sigma_C v_C}{\Delta s_C}\right]\delta\left(\frac{1}{l}\right) \qquad \text{(AI.14)}$$

As above, the entropies are approximated by Equation AI.9. On integration, all parameters are assumed to be constant as above. Finally one obtains

$$P(l) - P_0 = \frac{2\sigma_M v_M}{\Delta v_M}\left\{\frac{[(\sigma_C/\Delta H_C)/(\sigma_M/\Delta H_M)]-1}{[(\Delta v_C/v_C\Delta H_C)/(\Delta v_M/v_M\Delta H_M)]-1}\right\}\frac{1}{l} \qquad \text{(AI.15)}$$

or, equivalently

$$P(l) = P_0(1 - l_P/l) \qquad \text{(AI.16)}$$

where

$$l_P = \frac{2}{P_0}\frac{\sigma_M v_M}{\Delta v_M}\left\{\frac{[(\sigma_C/\Delta H_C)/(\sigma_M/\Delta H_M)]-1}{1-[(v_M \Delta H_M/\Delta v_M)/(v_C \Delta H_C/\Delta v_C)]}\right\} \qquad \text{(AI.17)}$$

The change of triple-point temperature and pressure with size for a particular system can now be evaluated with the help of Equations AI.12 and AI.16. The characteristic lengths l_T and l_P give typical thicknesses up to which the triple-point temperature and pressure, respectively, are depressed significantly.

An inspection of the expressions for the characteristic lengths reveals that a singularity appears if the following condition on the bulk quantities is fulfilled

$$v_M \Delta H_M/\Delta v_M = v_C \Delta H_C/\Delta v_C \qquad \text{(AI.18)}$$

and, at the same time, the ratio of the surface to bulk free energies of the crystal and mesophase are not equal, that is

$$\frac{\sigma_C}{\Delta H_C} \neq \frac{\sigma_M}{\Delta H_M} \qquad \text{(AI.19)}$$

Despite the fact that the above conditions appear to be stringent, it cannot be ruled out, *a priori*, that they may be fulfilled. In particular, Equation AI.18 is not unreasonable, since the heat of fusion is related empirically to the difference in specific volume, Δv, whereas the absolute specific volumes do not differ much (see Table AI.1). Furthermore, Equation AI.19 is likely to be true following the considerations in the main paper.

A caution applies, however, due to the assumptions and simplifications which have entered the above calculations. In particular, the temperature and pressure dependencies of the latent heats and specific volumes should lead to a temperature- and pressure-dependent condition for the singularity which is unlikely to be fulfilled over a range of T and P.

If, however, such a singularity does indeed persist, and both Equations AI.18 and AI.19 are fulfilled, then the characteristic lengths and both the triple-point temperature and the triple-point pressure go to zero.

Values for the various parameters in the case of PE with error margins are given in Table AI.1. It is evident from inspection of the error margins and Equations AI.13 and AI.17 that the error in the predicted triple point will be very large, even without consider-

TABLE AI.1

T_0	393 K	
P_0	3.3 kbar	
	Low pressure	High pressure
σ_C	$90 \pm 10 \times 10^{-3}$ J m^{-2} [2]	$44 \pm 10 \times 10^{-3}$ J m^{-2} [4]
ΔH_C	285 ± 10 J cm^{-3} [2]	380 ± 10 J cm^{-3} [3]
v_C	1.03 ± 0.02 cm^3 g^{-1} [5]	0.96 ± 0.02 cm^3 g^{-1} [3]
Δv_C	0.24 ± 0.02 cm^3 g^{-1} [5]	0.11 ± 0.02 cm^3 g^{-1} [3]
σ_M	$37 \pm 5 \times 10^{-3}$ J m^{-2} [2]	$6 \pm 2 \times 10^{-3}$ J m^{-2} [4]
ΔH_M	150 ± 20 J cm^{-3} [2]	120 ± 10 J cm^{-3} [3]
v_M	1.13 ± 0.02 cm^3 g^{-1} [5]	1.03 ± 0.02 cm^3 g^{-1} [3]
Δv_M	0.14 ± 0.02 cm^3 g^{-1} [5]	0.04 ± 0.02 cm^3 g^{-1} [3]

TABLE AI.2

	l_T (nm)	l_P (nm)
Low-pressure data	14.1	5.0
High-pressure data	2.0	1.8
High P, $\Delta H_M = 126$ J cm^{-3}	6.4	6.2
High P, $\Delta H_M = 127$ J cm^{-3}	10.0	9.8
High P, $\Delta H_M = 128$ J cm^{-3}	22.5	22.4

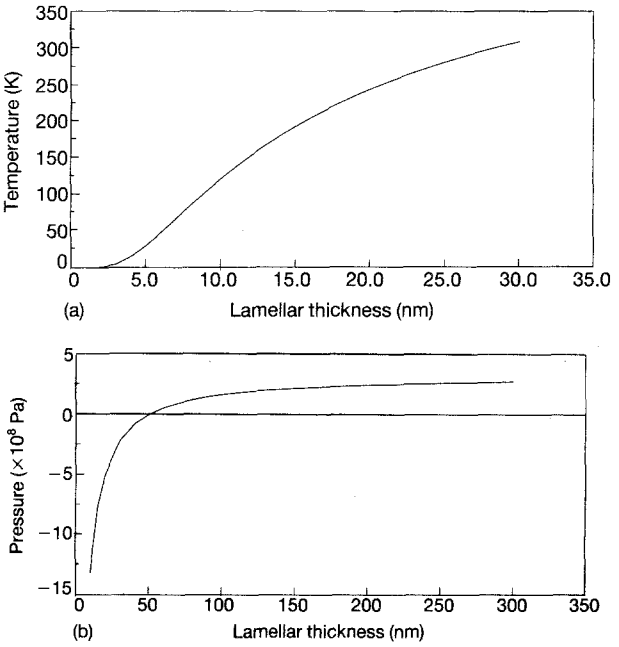

Figure AI.1 Variation of (a) the triple-point temperature and (b) the pressure with lamellar thickness for the parameter values given in Table AI.1 (low-pressure case, IT = 14.1 nm and Ip = 5 nm).

ing the approximations of constant parameter values made in the integration above.

Table AI.2 lists values of l_P and l_T which have been calculated with typical values of the parameters from Table AI.1. Both l_P and l_T are typically of the order of tenths of nanometres, unless the parameter values are chosen such that the singularity of Equation AI.18 is approached. This can be achieved with reasonable values of the parameters. Therefore the lengths l_T and l_P of the order of 100 nm, and hence a triple-point depression for crystals of that size down to ambient conditions cannot be ruled out (see Figs AI.1a and b).

References

1. R. DEFAY, I. PRIGOGINE, A. BELLEMANS and D. H. EVERETT, "Surface tension and adsorption", (Longmans, London, 1966).
2. Main text of the present paper.
3. W. DOLLHOPF, Thesis, University of Ulm, Germany (1979).
4. M. HIKOSAKA, Appendix III to this paper.
5. A. S. VAUGHAN, G. UNGAR, D. C. BASSETT and A. KELLER, *Polymer* **26**, (1985) 726.

Appendix II: Rates of growth of stable and metastable phases

This appendix aims to provide a map of the relative rates at which two competing phases develop, one being the stable phase, the other the metastable phase, at given conditions of temperature and pressure. The relation between relative stability and rates of growth has been considered before (see [1], and the references in the main paper), most recently by Cardew and Davey [2]. None of the above cases, however, considers the case of polymer crystallization, where the growth-rate equation takes the following form

$$N_{\text{meta}} = \alpha_{\text{meta}} \exp\left[\frac{-\beta_{\text{meta}}}{T(\Delta T)_{\text{meta}}}\right] \quad \text{(AII.1)}$$

$$N_{\text{stable}} = \alpha_{\text{stable}} \exp\left[\frac{-\beta_{\text{stable}}}{T(\Delta T)_{\text{stable}}}\right] \quad \text{(AII.2)}$$

where α, β and ΔT are as defined in the main text. In order to get an overview of the competition between the two phases as a function of temperature, the rate parameters α and β have been chosen to comprise the cases $\alpha_{\text{meta}} < \alpha_{\text{stable}}$, $\alpha_{\text{meta}} = \alpha_{\text{stable}}$, and $\alpha_{\text{meta}} > \alpha_{\text{stable}}$, with $\beta_{\text{meta}} < \beta_{\text{stable}}$ and $\beta_{\text{meta}} > \beta_{\text{stable}}$ (see Table AII.1). The values of the exponential factor, β, have been chosen to be of the same order of magnitude as in the case of secondary nucleation of PE. The values of the pre-exponential factor, α, are meant to reflect the ratios of the attachment frequencies which the two different phases might have. They are not scaled to any particular magnitude of N, however. The melting points of the two phases are fixed at $(T_m^\circ)_{\text{meta}} = 410$ K and $(T_m^\circ)_{\text{stable}} = 420$ K resulting in

$$(\Delta T)_{\text{meta}} < (\Delta T)_{\text{stable}} \quad \text{(AII.3)}$$

at any temperature. Hence, as mentioned in the main paper, the effects of supercooling and the factor β oppose each other if $\beta_{\text{meta}} < \beta_{\text{stable}}$, leading to a cross-over of the rates close to the melting point, for any choice of α (see Figs AII.1–AII.3). The metastable phase then becomes the kinetically preferred phase for lower temperatures, unless the pre-exponential frequency factor is sufficiently larger for the stable phase. As displayed in Fig. AII.3 this leads to a second cross-

TABLE AII.1 Parameter values of the rate equations for metastable and stable phases

Figure	α_{meta}	α_{stable}	β_{meta} (K^2)	β_{stable} (K^2)
AII.1	3	1	30000	60000
AII.2	1	1	30000	60000
AII.3	1	3	30000	60000
AII.4	3	1	60000	30000
AII.5	1	1	60000	30000
AII.6	1	3	60000	30000

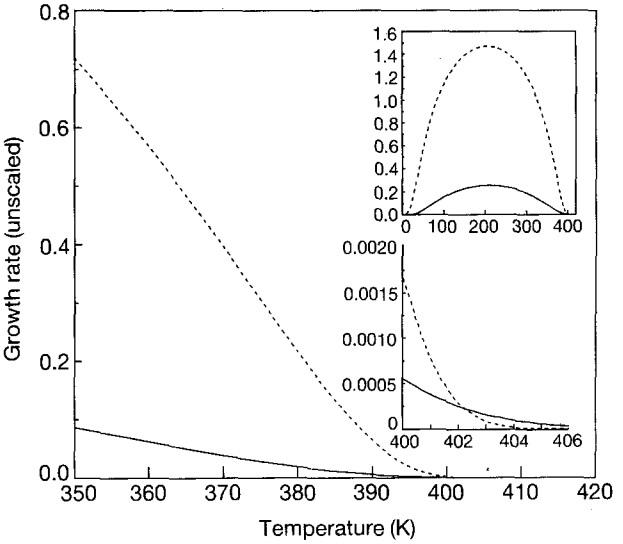

Figure AII.1 The growth rate as a function of the temperature of two phases according Equations AII.1 and AII.2 for the values of the parameters given in Table (AII.1. (---) Meta, and (——) stable. The main graph shows the temperature region which is generally of most interest to the experimental situation. The insets show the full temperature range from 0 K to the melting point, and (where appropriate) the region of the cross-over near the melting point.

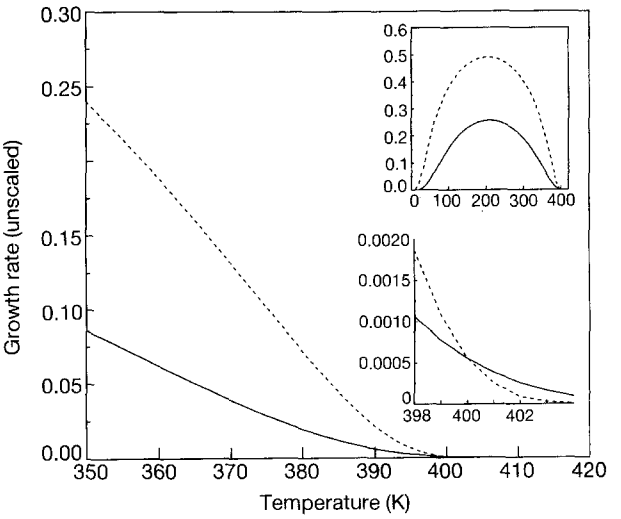

Figure AII.2 (---) Meta, and (——) stable. See Fig. AII.1 and Table AII.1.

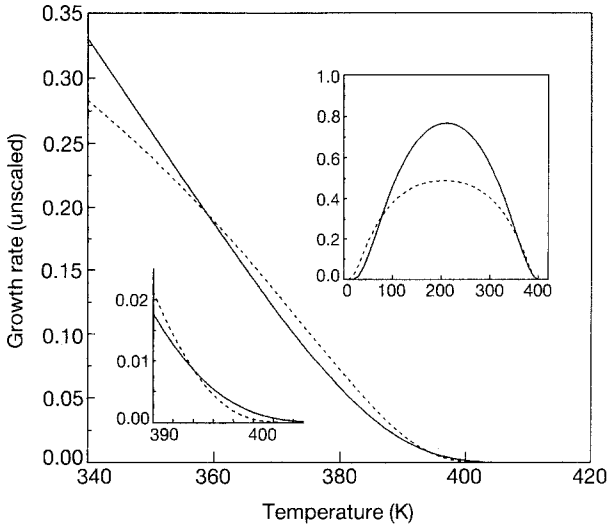

Figure AII.3 (---) Meta, and (——) stable. See Fig. AII.1 and Table AII.1.

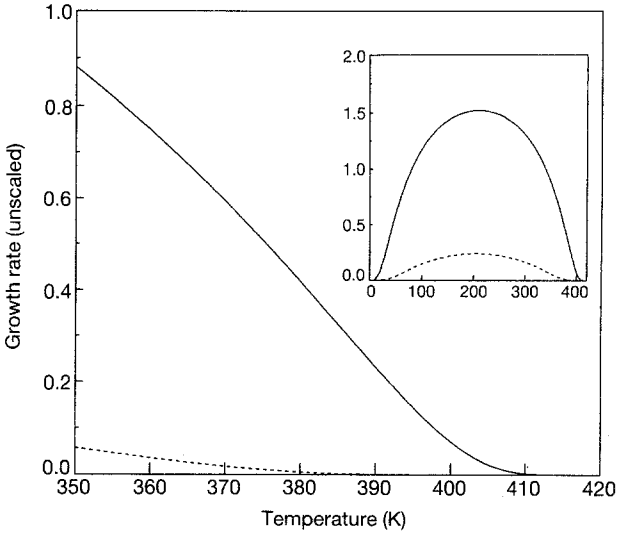

Figure AII.6 (---) Meta, and (——) stable. See Fig. AII.1 and Table AII.1.

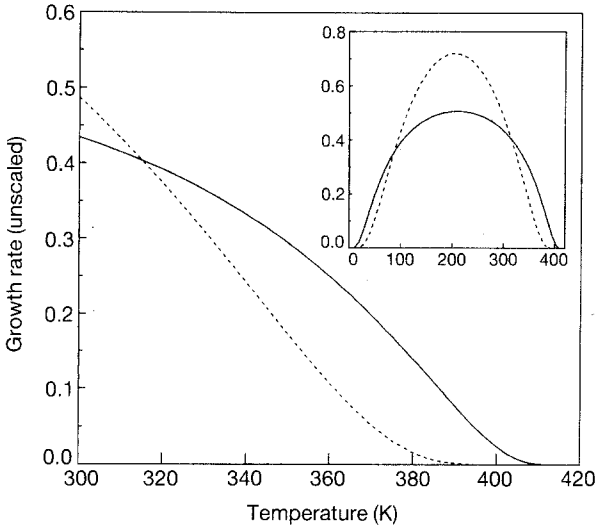

Figure AII.4 (---) Meta, and (——) stable. See Fig. AII.1 and Table AII.1.

over at a supercooling of around 50 K, when the stable phase becomes the fastest phase once again. It is, however, unlikely that the phase with higher thermodynamic stability has a higher attachment probability than a less stable phase. This would mean a higher entropy, which, in turn, opposes stability. Figs AII.4–AII.6 display the cases where $\beta_{meta} > \beta_{stable}$, in contrast to the examples studied in the main paper. The diminished likelihood of the situations represented by these curves is discussed in the main text. On both counts, the physically most likely case is therefore that displayed in Fig. AII.1.

References

1. R. DEFAY, I. PRIGOGINE, A. BELLEMANS and D. H. EVERETT, "Surface tension and adsorption", (Longmans, London, 1966).
2. P. T. CARDEW and R. J. DAVEY, "Tailoring of crystal growth", Conference of the British Association of Crystal Growth, Institute of Chemical Engineers, North Western Branch, Manchester, UK (Inst. Civil Eng., 1982).

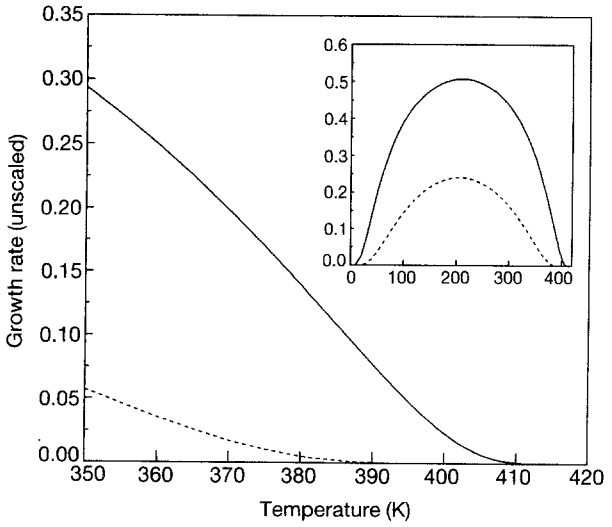

Figure AII.5 (---) Meta, and (——) stable. See Fig. AII.1 and Table AII.1.

Appendix III. A comparison of the values for the surface free energy of hexagonal and orthorhombic polyethylene crystals

This appendix is based on the theory of sliding diffusion proposed by one of the authors (M, H)[1, 2]. It explains the supercooling, ΔT, dependence of the lateral growth rate, V, and the lamellar thickness of folded-chain and extended-chain crystals. It will briefly be outlined how the values of surface free energies of h- and o-crystals can be estimated from an analysis of the observed values of V and l [3, 4].

In the theory of crystallization, growth has been described by a sequential process, and any growth rate can be related to a net flow, j, of the sequential process. In [2], j was formulated as a function of a path parameter, ω, that is, $j(\omega)$. The latter represents the shape of a crystal or nucleus [1, 2]. Since j can be

TABLE AIII.1 Parameters obtained from analysis of the dependence on the degree of supercooling, ΔT, of l and the lateral growth rate, V, for orthorhombic (o) and hexagonal (h) crystals of PE [2–4]

	Set I (orthorhombic at 0.1 MPa)	Set II (hexagonal at 0.3 GPa)
σ (10^{-3} J m^{-2})	10.9	3.3
σ_e (10^{-3} J m^{-2})[a]	43.9	6.3
κ (kT_m per repeating unit)	0.66	0.35

[a] Calculated from equation 13 in [2].

regarded as a weight of a possible growth path, an average of any physical quantity, X, can be defined by

$$\langle X \rangle = \frac{\int X j(\omega)\, d\omega}{\int j(\omega)\, d\omega} \quad \text{(AIII.1)}$$

It is natural to consider that $\langle X \rangle$ can be compared with the observed X. In the present case, V and l have been formulated as functions of j, thus we have $\langle V \rangle$ and $\langle l \rangle$, which can be compared with the observed V and l. $\langle V \rangle$ is, for small ΔT, given by [4, 5]

$$\langle V \rangle \sim \exp(-\Delta E_e^*) \exp(-G^*/I)\Delta T \quad \text{(AIII.2)}$$

where ΔE_e^* is the activation free energy for sliding diffusion within a critical nucleus, and G^* is the critical free energy of a two-dimensional nucleus, I is a constant (1 for single nucleation, 2 or 3 for multinucleation). The term ΔT is due to the so called "survival probability". $\langle V \rangle$ has been shown to be determined by two parameters; one is the side-surface free energy, σ, and the other is a parameter which describes the activation energy of chain sliding diffusion ($\kappa = \nu$) [1, 2]. l is assumed to be

$$l = A' n^{1+\omega} \quad \text{(AIII.3)}$$

where A' is a constant given by equation 21 in [5] and n is the number of stems within the nucleus. $\langle l \rangle$ contains three parameters: σ, κ and N/N^*, where N and N^* are the number of repeating units within a nucleus and the number within a critical nucleus, respectively, [3, 4]. It is to be noted that the end-surface free energy, σ_e, can be derived from σ by using Equations 4, 5 of [5].

Thus σ and κ of o- and h-crystals were obtained by comparing $\langle V \rangle$ and $\langle l \rangle$ with the observed V and l [2, 3, 4]. The result is shown in Table AIII.1. In this analysis, the only remaining parameter is N/N^*, which was assumed to be 100. The result does not depend significantly on its exact value, however.

We can see from Table AIII.1 that $(\sigma_e)_h \sim 1/7(\sigma_e)_o$. As $(\Delta H)_h \sim 1/2(\Delta H)_o$ the contention that

$$\left(\frac{(\sigma_e)_h}{\Delta H}\right)_h < \left(\frac{\sigma_e}{\Delta H}\right)_o$$

is upheld.

References

1. H. HIKOSAKA, *Polymer* **28** (1987) 1257.
2. *Idem. ibid.* 31 (1990) 458.
3. *Idem.* First Conference on Advanced Topics in Polymer Science 1988 (Italy), Europhys. Conf. Abs. 1988, 12D, 76.
4. M. HIKOSAKA, in preparation.
5. M. HIKOSAKA and T. SETO, *Jpn. J. Appl. Phys.* **23** (1984) 956.